Department of Biosciences and Nutrition
Center for Biotechnology
Karolinska Institutet, Stockholm, Sweden

THE DYNAMIC ENVELOPE OF A FUSION CLASS II VIRUS; MOLECULAR REORGANIZATIONS DURING PREFUSION STAGES OF SEMLIKI FOREST VIRUS

Lars Haag

Stockholm 2006

Cover illustration: "Snapshot of alphavirus acid activation" L. Hammar, watercolor 2002.
(Reprinted with permission from the publisher)

J Biol Chem Feb. 28, 2003, On the cover: from stable cool beauty at neutral pH to sliding worms in the acidic environment of the endosome. Alphaviruses carry an external protein shell where two membrane-anchored proteins are nested. Therefore, to allow a close encounter of virus and target membranes the shell architecture has to dissolve along with exposure of its endosequence fusion peptide. Lacking the helical motifs characterizing a Type I fusion mechanism these viruses represent a less well explored Type II triggering. Initial events of the process are followed by domain probing in real time by *Hammar, L., Markarian, S., Haag, L., Lankinen, H., Salmi, A. & Cheng, R. H., pp 7189-98.*

Published and printed by Karolinska University Press
Box 200, SE-171 77 Stockholm, Sweden

ISBN 91-7140-718-9

ABSTRACT

The aim of this study was to explore a membrane fusion mechanism, prevailing in alphaviruses and known as virus class II fusion. The model virus for this mechanism is Semliki Forest virus (SFV). Contrary to class I fusion, for which the influenza virus is the prototype along with HIV, class II fusion mechanism involves membrane proteins mainly folded in β-sheet structures, not α-helices as in the class I case.

The fusion class II viruses enter the cell by fusion with the endosomal membrane. Acidification is a prerequisite for the fusion step to occur and to fulfill the infection *in vivo*. Virus fusion can be triggered experimentally by acidification in the presence of a target membrane. The acidification would transform the virus into a fusogenic state, after which it is prone to interact with the membrane. Thus, by mimicking the environment in the endosome, stages in the fusion process can be studied under well-defined conditions.

In the present work I have focused on the dynamic transformation of SFV at stages preceding membrane fusion. To do so, the accessibility of functional domains in the virus envelope was explored with the aid of antibodies and various biochemical methods. Electron cryo-microscopy (cryo-EM) was used to capture intermediate forms of the virus. This provides data for three-dimensional (3D) structure determination to reveal details and fusion related variations. Pseudo-atomic resolution structures of the virus particle from combined x-ray and cryo-EM data enabled protein assignment to densities within the cryo-EM map. In addition, experiments with formaldehyde (FA) cross-linking of virus particles were performed to gain understanding of its morphological effects. The aim was to develop a method to safely prepare virus specimens for structural studies and, possibly, enhance structural details.

In the structures solved, details of acid-induced rearrangements were conclusively identified. The major changes occur as an expansion of the external domain. In the raised shell layer the expanded area show widened shell openings and dissolved protein contacts. In the stalks of the protruding spikes the two glycoproteins separate, but keep together in the spike head lobes, while in the sub-membrane domain the envelope contacts with the nucleocapsid (NC) is released. In spite of the essentially retained virus morphology, several antibody epitopes, including the receptor binding domain and the fusion loop, become exposed in a pH dependent manner. This implies that subtle local rearrangements might represent essential functional stages.

In summery, by exploring prefusion stages as they occur in a native virion, this thesis tries to fill a gap in knowledge on viral membrane fusion mechanisms. It shows details of the virus class II fusion mechanism not earlier discussed. It presents new observations and demonstrates sequential stages of rearrangements in the virus structural domains related to the adaptation of a fusogenic state. The results suggest a cooperative action between the two envelope proteins at stages beyond the control of fusion loop exposure. Furthermore, it also presents a procedure to safely prepare virus specimens for structural studies under close to native conditions.

LIST OF PUBLICATIONS

This thesis is based on the following papers, which are referred to in the text by their Roman numerals (I-IV).

I. Haag, L., Garoff, H., Xing, L., Hammar, L., Kan, S.-T., and Cheng R. H. Acid-induced movements in the glycoprotein shell of an alphavirus turn the spikes into membrane fusion mode (2002). *EMBO Journal*, 21, 4402-4410.2.

II. Hammar, L., Markarian, S., Haag, L., Lankinen, H., Salmi, A., and Cheng R. H. Prefusion rearrangements resulting in fusion peptide exposure in Semliki Forest virus (2003). *Journal of Biological Chemistry*, 278, 7189-7198

III. Wu, S.-R., Haag, L., Wu, B., Murata, K., Xing, L., Garoff, H., Hammar, L., and Cheng, R. H. The dynamic envelope of a fusion type 2 virus; detection of inter and intramolecular reorganizations during prefusion stages. *(Manuscript)*

IV. Haag, L., Sjöberg, M., Lindqvist, B., Garoff, H., Hammar, L. and Cheng R. H. Formaldehyde inactivated Semliki forest virus show preserved morphological and immunological features. *(Manuscript)*

CONTENTS

LIST OF ABBREVIATIONS

3D	Three-dimensional
aa	Amino acids
C	Capsid
BHK	Baby hamster kidney
Cryo-EM	Electron cryo-microscopy
Da	Dalton
DNA	Deoxyribonucleic acid
E1	Envelope protein 1
E2	Envelope protein 2
ELISA	Enzyme-linked immunosorbent assay
EM	Electron microcopy
ER	Endoplasmatic reticulum
FA	Formaldehyde
fab	Fragment antigen binding
GNA	Galanthus nivalis agglutinin
HA	Hemagglutinin
Ig	Immunoglobulin
MAb	Monoclonal antibody
NC	Nucleocapsid
PFT	Polar Fourier transform
PM	Plasma membrane
RNA	Ribonucleic acid
SDS-PAGE	Sodium dodecyl sulfate polyacrylamide gel electrophoresis
sE1	Soluble E1
SFV	Semliki Forest virus
SIN	Sindbis virus
SPR	Surface Plasmon resonance
T	Triangulation number
TBE	Tick-borne encephalitis virus
TM	Transmembrane
Tris	Tris hydroxymethylaminoethane
WB	Western blot
wt	Wild-type
Å	Ångström

1 INTRODUCTION

Viruses are pathogens and are considered non-living organisms (*i.e.* not capable to replicate without a host cell). They are, therefore, simply cellular parasites. The virus infects new cells by transmitting its genetic information packaged in a transport carrier, which after release from the host cell, is spread by various routes to find new target hosts. The fragile genetic information, which is either in the form of RNA or DNA, must be protected during the extracellular phase. Different strategies have been developed among viruses to protect their delicate cargo. This usually includes a protective shield in the form of at least one layer of protein and some viruses also possess a lipid bilayer. The outermost protein layer carries the recognition molecule for host-cell receptor/receptors which allows the virus to adhere to the host. Moreover, the protective proteinaceous shield requires a dynamic construction since it at some point during the life-cycle, needs to be disentangled in order to release its infectious content into the targeted hosts. Enveloped viruses, containing a lipid membrane, carry proteins on their surface with the ability to recognize, adhere and subsequently induce membrane fusion of suitable target cells. For these reasons the exterior of the virus carries proteins with multiple functions.

The life-cycle of a virus can be divided into several steps; attachment, internalization, transcription/translation, replication, assembly, release and transport through the extracellular phase to new targets. Cell entry involves the binding of the virus to a predefined cell receptor/receptors followed by internalization. The virus is usually adapted to a more or less specific cellular structure for entry. Internalization can occur directly at the plasma membrane (PM) or after endocytosis. Once inside the cell, the genome must be translated so that new viral proteins can be synthesized and the genome replicated. During the last step new virus particles are assembled and released to be spread and infect new hosts. The release of virus particles occur either internally followed by cell lysis, or by budding directly at the PM. Once outside the cell, the search to infect new hosts begins and often includes complicated routes of infection. The present study focus on virus entry by membrane fusion, highlighting the specific and complicated molecular reorganizations involved in converting the stable transport particle into a fusogenic state.

1.1 ALPHAVIRUS

Alphavirus was originally classified as a Flavivirus but was later re-evaluated and moved into a separate group. It is a relatively small virus with a positive single stranded RNA (ssRNA) that today belongs to the alphavirus genus in the Togaviridae family (http://www.ncbi.nlm.nih.gov/ICTVdb/Ictv/index.htm). Members of the alphavirus family can cause symptoms such as fever, rashes, arthritis and encephalitis (Schlesinger & Schlesinger, 2001, Shope, 1980). Several members of the alphaviruses are potential threats both to humans and to domestic animal stocks where outbreaks can have economical consequences. An outbreak of Chikungunya virus, in the alphavirus family,

on the islands of Réunion east of Madagascar has been reported with thousands infected (www.smittskyddsinstitutet.se). Owing to its generally low pathogenicity and ease of expression in cell cultures, alphavirus has been used as a prototype virus in studies of biologically relevant processes such as virus membrane fusion and assembly (Garoff et al., 2004, Kielian, 1995, Strauss & Strauss, 1994). The alphaviruses have a relatively simple but rigid construction which follows icosahedral symmetry. This has allowed the structural determination for several members in the alphavirus genus such as Semliki forest (SFV), Sindbis (SIN), Ross River and Aura virus (Cheng et al., 1995, Mancini et al., 2000, Zhang et al., 2002a, Zhang et al., 2002b). The dynamic properties of the virus particle have been studied *in vitro* under conditions triggering biologically relevant events. These events, mimicked *in vitro*, include molecular reorganizations occurring during the membrane fusion process. These events have been studied using antibody binding assays, mutational analyses, trypsin sensitivity and changes in oligomerization states of the viral proteins (Kielian, 1995). Furthermore, molecular reorganizations have also been studied structurally using electron cryo-microscopy (cryo-EM) (Fuller et al., 1995, Haag et al., 2002, Paredes et al., 2004). Today it is well established that the alphavirus goes through a series of intermediate conformational stages prior to membrane interaction and fusion. However, the exact mechanism is still not fully understood.

1.2 STRUCTURE OF ALPHAVIRUS

SFV is an alphavirus isolated from mosquitoes found in the Semliki Forest in western Uganda. It is an enveloped virus with icosahedral symmetry and triangulation number (*T*) of four, as seen in 3D reconstructions of native virions (Haag et al., 2002, Mancini et al., 2000). The virus surface is decorated with 80 triangular-shaped spike-like protrusions projecting about 10 nm from the outer lipid bilayer giving the whole virion a total diameter of about 70 nm (**Fig. 1**). The $T = 4$ symmetry implies that 60 of the spikes are located at the quasi 3-fold and 20 at icosahedral 3-fold axes. A 4-5 nm thick lipid bilayer is found between the outer glycoprotein layer composed of the envelope proteins 1 (E1) and 2 (E2) and the underlying nucleocapsid (NC). The internal NC is composed of capsid protein (C) monomers arranged as hexamers and pentamers according to same T=4 icosahedral symmetry found for the surface spikes (**Fig. 1**, lower right). The diameter of the NC is approximately 40 nm. The N-terminus of the C protein is located towards the center of the particle and interacts with the viral RNA while the globular C-terminus facing the inner lipid layer binds to the external spike layer via its connection to the E2 protein (Cheng et al., 1995, Garoff & Simons, 1974, Skoging & Liljestrom, 1998, Skoging et al., 1996).

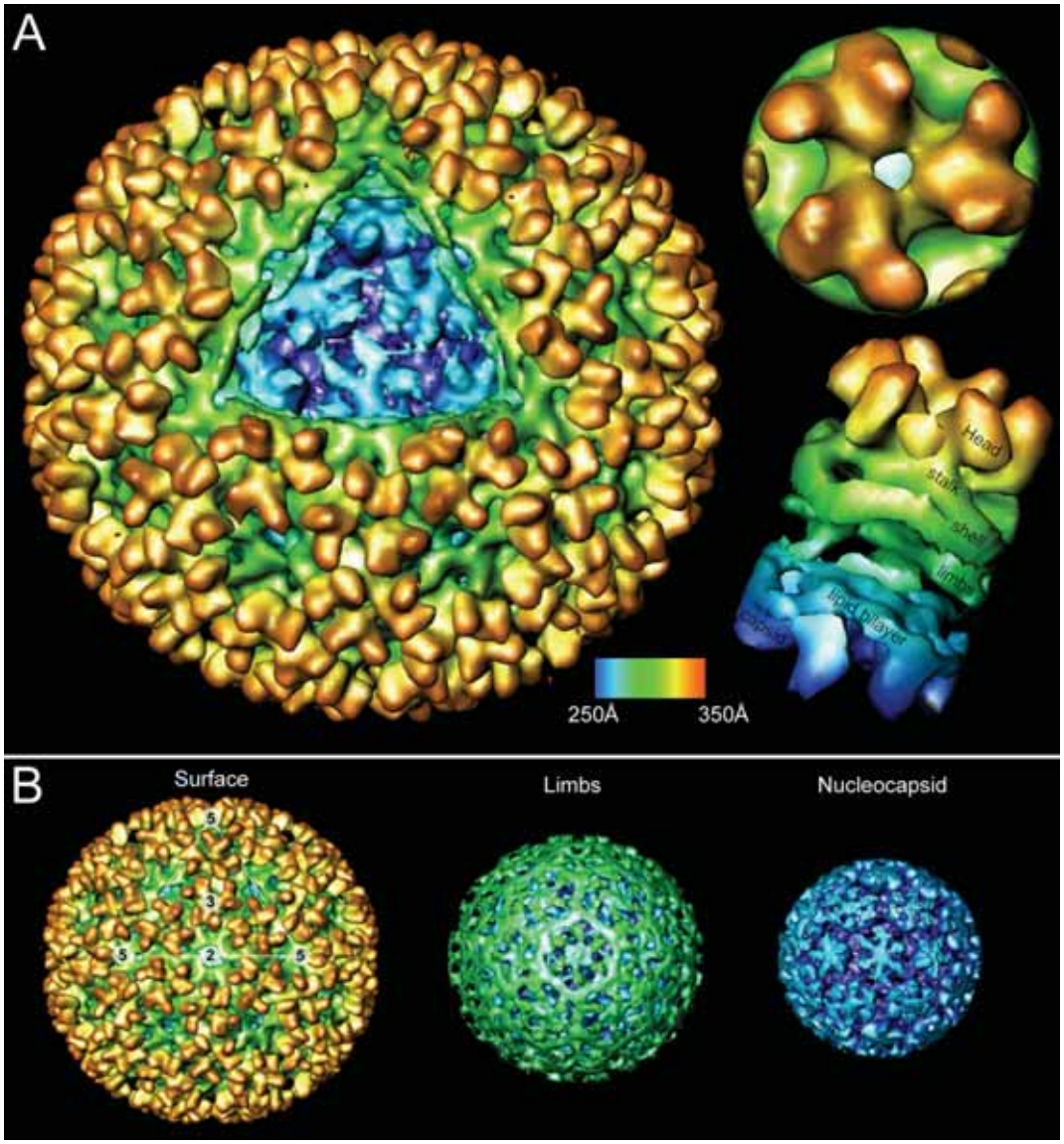

Figure 1. *Cryo-EM density map of SFV.* Three dimensional structure of SFV as reconstructed from electron cryo-EM micrographs to 28 Å resolution. A cut-open 2-fold view (one face of the icosahedron has been removed) of SFV displaying the interior of the virus and radially color coded as described in the legend. Top (A, top right) and side (A, bottom right) view of a 3-fold E1/ E2 glycoprotein spike as cut out from the reconstruction with labels for the different layers. Two-fold surface view of the SFV over-layered with the respective 2-, 3-, and 5-fold symmetry axes (B, left). Radial cuts of the SFV show the limbs and lipid bilayer (B, middle) and the NC (B, right).

Today, substructures such as the C protein and the ecto-domain of the E1 protein have been solved to atomic resolution using x-ray crystallography (Choi et al., 1997, Lescar et al., 2001). With these atomic resolution structures available, it has been possible to build pseudo-atomic virus models by fitting them into the framework of cryo-EM density maps (Mancini et al., 2000, Zhang et al., 2002b). Analysis of internal protein interactions in these pseudo atomic virus structures have helped to better understand the intricate protein organization. Protein domains believed to be involved in specific biological functions have also been suggested. Furthermore, un-assigned densities after the modeling suggest the position and shape of the still structurally undetermined E2 protein (Zhang et al., 2002b). Structural characterization of the virus organization has also been assessed using probes such as fragments antigen binding (fab) and heparin

(Smith et al., 1995, Zhang et al., 2005). Another way to localize the position of E1 and E2 comes from sugar site mutations. Three-dimensional SIN reconstructions revealing the mutation sites in the E1 and E2 proteins have been determined from the organization of the glycoproteins could be traced (Pletnev et al., 2001).

1.2.1 Structural proteins and their functions

Members of the alphavirus family are composed of the following structural proteins; the C protein, the p62 precursor protein, 6K and the E1 protein. The structural proteins are translated as a single poly-protein precursor in the following order C-p62-6K-E1. The C protein (33 kDa) carries autoproteolytic activity and cleaves itself off from the polyprotein during translation (Aliperti & Schlesinger, 1978, Melancon & Garoff, 1987). The C protein also contains a stretch of positively charged amino acids (aa) at the N-terminus with RNA binding properties (Forsell et al., 1995, Garoff et al., 1980a, Geigenmuller-Gnirke et al., 1993, Weiss et al., 1994, Weiss et al., 1989). Proteolytic cleavage by a cellular furin-like protease of the p62 protein generates the E2 (52 kDa) and E3 (10 kDa) proteins (Jain et al., 1991). The cleavage is crucial for priming the acid sensitivity of the virus and hence infectivity (Lobigs & Garoff, 1990, Salminen et al., 1992, Tubulekas & Liljestrom, 1998). Following the p62 protein are the small 6K protein (6 kDa) protein and the E1 glycoprotein (49 kDa). The 6K protein occurs in non-stoichiometric amounts compared to the E1 and E2 proteins in the mature virus particle (Gaedigk-Nitschko & Schlesinger, 1990, Lusa et al., 1991). Mutagenesis within the 6K protein leads to a deficiency in assembly and budding, indicating that the 6K protein is somehow involved at a late stage in the assembly process (Gaedigk-Nitschko & Schlesinger, 1990, Liljestrom et al., 1991, Loewy et al., 1995, Lusa et al., 1991).

The heterodimeric glycoproteins E1 and E2 are non-covalently but tightly interconnected as trimers, observed as the tri-lobed spikes on the virus surface. The small E3 protein is believed to be non-covalently associated with the SFV particle but absent in other alphaviruses such as Sindbis virus (Mayne et al., 1984, Welch & Sefton, 1979). The envelope proteins carry one or more glycosylation sites shown to be important for the stability of the oligomer (Wengler & Rey, 1999). They carry biological functions such as receptor recognition as well as mediating the membrane fusion. While the E2 protein is involved in the initial binding to the host cell, the E1 protein carries the cell membrane insertion loop at aa Asp 79 and Asp 97 (Garoff et al., 1980b, Gibbons et al., 2004a, Levy-Mintz & Kielian, 1991). E1 is further involved in the subsequent merging of viral and host cell membranes during the fusion step. Forces maintaining the overall particle integrity are mainly the external, lateral interactions of the E1 protein as seen from E1 modeling studies. The E2 protein is the linker between the external glycoprotein layer and the underlying NC. This linkage is mediated by a 31 aa long sub-membrane cytoplasmic domain often referred to as the E2-tail.

1.2.2 Virus structural tour; exterior to interior

The non-covalently interconnected E1 and E2 transmembrane (TM) proteins and the peripheral E3 polypeptide, which form the virus spikes, are often subdivided into the spike head, stalk, shell, and limb domains (joint E1 and E2 density leading to the lipid bilayer) (**Fig. 1**, top right). The bulk of the protruding part of the spike is believed to be composed mainly of the E2 protein (head). The domain between the spike head and the shell domain will be referred to here as the stalk (sometimes referred to as the stem). Following the stalk region is the shell layer (or skirt), which is mainly composed of extensive lateral *inter*-E1 contacts. The shell layer, surrounding the lipid bilayer, contains apparent openings at the 2- and 5-fold axes (**Fig. 1**, lower left). The E1 and E2 proteins join underneath the shell domain forming the limbs that traverse the lipid bilayer as tilted α-helical dimers (Mancini et al., 2000, Mukhopadhyay et al., 2006). The E2 protein carries three palmitoylated cysteines on the sub-membrane E2-tail which are anchored into the viral lipid bilayer (Ivanova & Schlesinger, 1993, Schmidt et al., 1979). Furthermore, aromatic aa in the cytoplasmic tail bind to a hydrophobic pocket in the globular folded C-terminus of the C protein, establishing a one-to-one connection between the outer glycoprotein spikes and the NC (Owen & Kuhn, 1996, Skoging et al., 1996, Zhao et al., 1994). It is this one-to-one connection between the outer spike layer and the NC that connects the *T*=4 icosahedral symmetry of both these protein layers. Finally, the highly positively-charged N-terminal domain of the C protein binds nonspecifically via charge neutralization to the internally located and protected viral RNA.

1.2.3 Model fitting of the viral structural proteins

Crystal structures of the C-terminal domain of the capsid protein of both SFV and SIN have been solved to atomic resolution (Choi et al., 1997, Choi et al., 1991). Fitting these models into the cryo-EM structure of the virion has helped in understanding the interactions involved the formation of the NC (Cheng et al., 1995, Mancini et al., 2000, Rossmann, 2000, Zhang et al., 2002b). The C protein binds both laterally to neighboring capsid proteins as well as vertically to the tail of the E2 protein. Studies on SFV mutants show that the conserved motif Tyr-X-Leu in the E2 sub-membrane domain binds to a hydrophobic cavity in the C protein and that the establishment of this interaction is crucial for the assembly of the virus particles (Skoging et al., 1996, Skoging-Nyberg & Liljestrom, 2000).

A soluble ectodomain of the E1 protein is another of the SFV structural proteins whose structure has been solved to atomic resolution by x-ray crystallography (Lescar et al., 2001, Roussel et al., 2006) (**Fig. 2A**) . Detergent extraction of purified virus particles produced so called “rosettes” composed of the E1 and E2 proteins, and these have been proteolytically cleaved into soluble E1-E2 dimers. After deglycosylation these dimers form crystals containing only the soluble E1 ectodomain, hereafter referred to as sE1 (Wengler & Rey, 1999). The atomic resolution structure of sE1 was solved and shows similar rod-shaped structure (**Fig. 2A**) mainly composed of β-sheets to the soluble ectodomain of the E protein from tick-borne encephalitis virus virus (TBE) of the

flaviviruses (Rey et al., 1995). The atomic resolution structure of the sE1 protein fit in a back-to-back and head-to-tail orientation at the local 2-fold axis when modeled into a 9Å SFV reconstruction (Lescar et al., 2001), similar to what is shown in **Figure 2B**. The sE1 protein lines up in an oblique orientation along the outer stalk of the trilobed spike and constitutes most of the shell domain. In this orientation, the fusion peptide is hidden underneath the proposed E2 density in the spike head. The other end of the molecule, with its Ig-like domain (domain III), sits around the openings at the 2- and 5-fold axes. In another study, the positions of E1 and E2 glycosylation sites were used as additional restraints for fitting the E1 model into an 11Å SIN reconstruction (Pletnev et al., 2001) but did not deviate markedly from the earlier study. Moreover, based on the sE1 position, both the shape and position of the E2 protein was proposed from difference mapping (Zhang et al., 2002b). This work shows that the E2 protein constitutes most of the spike head and the internal density of the spike. To a large extent, the E2 density also shields the E1 protein, in particular the fusion loop, from external accessibility. The proposed E2 location is supported by a structural study where fabs was used to localize the presumed receptor binding domain in the E2 protein (Smith et al., 1995). In that study they show that the proposed receptor binding domain is located at the outermost tip of the tri-lobed leaflets of spike.

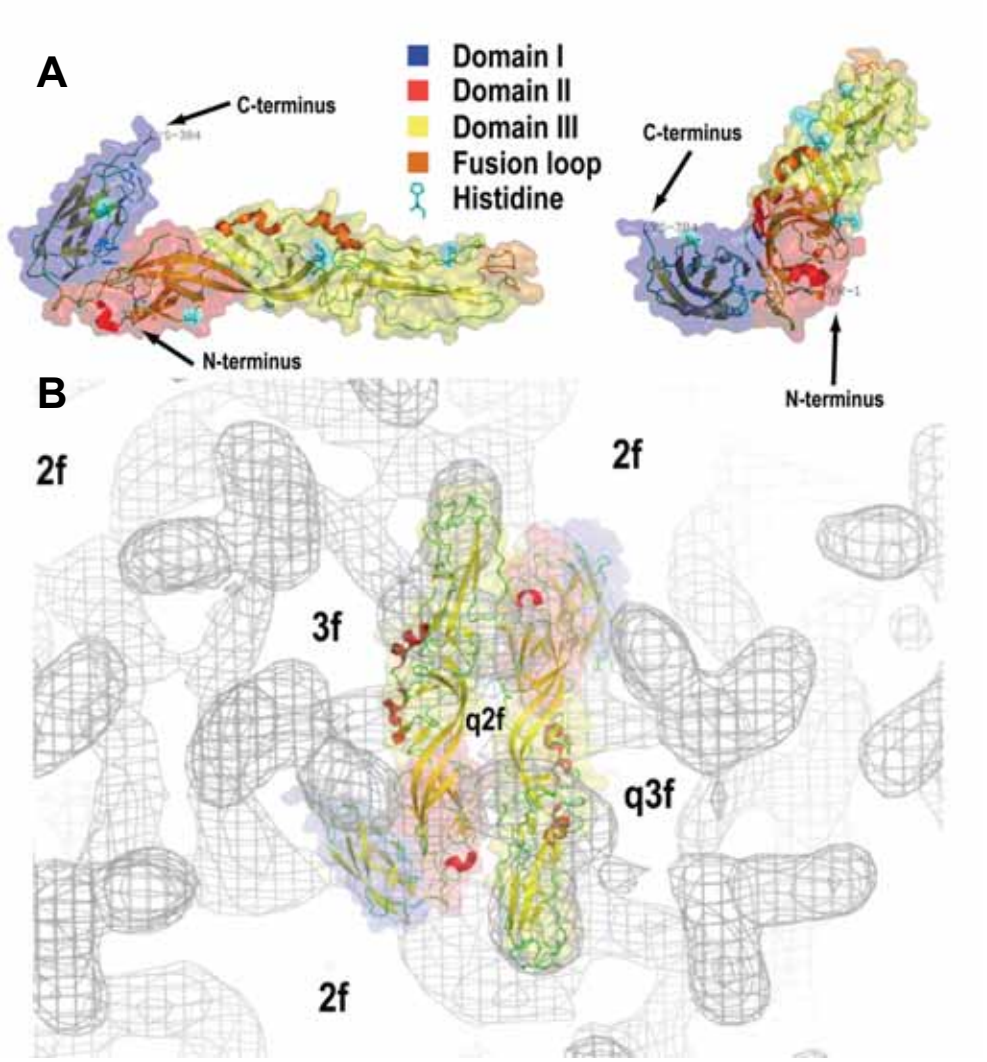

Figure 2. *The atomic resolution structure of E1 and model fitting into the SFV cryo-EM density map.* Top and side view of the atomic structure of the monomeric soluble E1 ectodomain (PDB_ID:2ALA, (Roussel et al., 2006). (A) A semi-transparent isosurface is over-layered emphasizing the domain I (blue), II (red) and III (yellow), as well as the fusion loop (orange). α-helices (red), β-strands (yellow) and loops (green) as well as the positions of the histidines and the C- and N-terminus are also shown. The E1 molecule as seen from a top view (upper left) or as viewed from a 2-fold axis of the obliquely positioned molecule with the fusion loop facing inwards (upper right). (B) Atomic resolution structure of the E1 molecule model fit into the density of a SFV cryo-EM reconstruction. The E1 position is in dimeric contact, at the quasi 2-fold axis, to the E1 belonging to the neighboring quasi 3-fold spike. Domain III aligns around the 2-fold axis while the fusion loop hides in a shielded location under the head of the spike.

1.3 ALPHAVIRUS LIFE-CYCLE

Infection by the alphavirus begins with the attachment to a host cell receptor/receptors followed by internalization via endocytosis. During the endocytic pathway, acidic pH in the endosomes triggers conformational changes within the virion. This ultimately leads to the merger of the virus and host cell membranes and to the subsequent release of the viral genome. Translation of the non-structural proteins and subsequent synthesis of the structural proteins takes place exclusively in the cytoplasm. After replication of the genome, assembly and finally budding of the virus particles take place at the PM. A schematic picture of the life-cycle is shown in **Figure 3**.

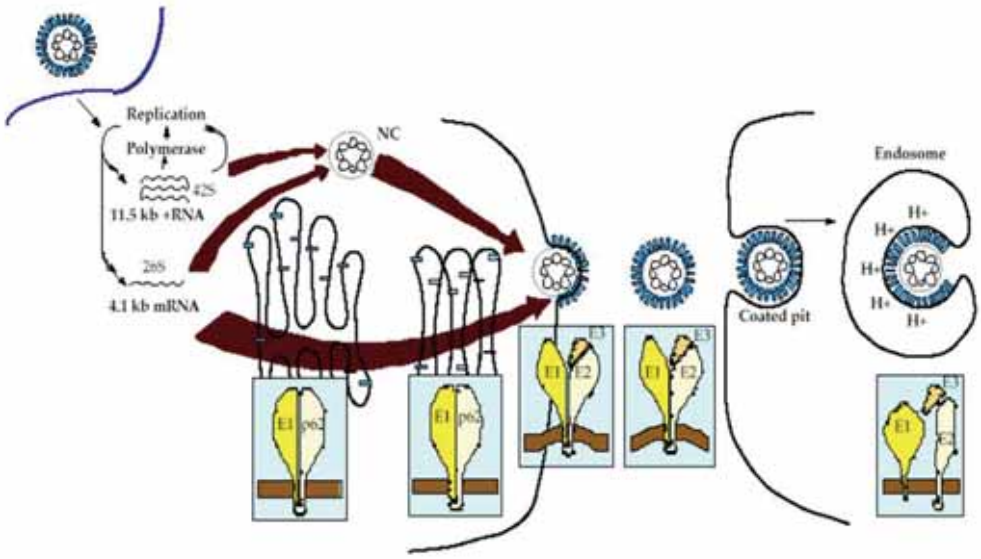

Figure 3. *Alphavirus life cycle.* A schematic overview of the different stages during the alphavirus life-cycle. Shown also is a cartoon of the maturation of the structural glycoproteins E1, p62, E2 and E3. The right hand side depicts virus entry into the host via the receptor-mediated endocytosis. Acid pH triggers virion structure rearrangement, ultimately leading to membrane fusion and NC release. Shown on the left hand side is the translation and replication of the positive 42S ssRNA. All the structural proteins are translated from a sub-genomic 26S RNA in the order C-p62-6K-E1. After release of the C protein, the remaining spike glycoproteins are processed in the ER and transported via the cell's secretory pathway to the PM. The C protein encapsidates newly synthesized viral RNA forming NC's. During the transport to the PM the p62 is proteolytically cleaved into the mature acid sensitive form E2 and E3. The spike glycoproteins associate with preassembled NC's on the PM and budding of new virions take place.

1.3.1 Entry

Virus cell entry can be endocytic or non-endocytic. The non-endocytic entry includes direct fusion at the PM, pore formation and cell-cell induced fusion. Viruses which rely on internalization via the endosomal route can be further subdivided into clathrin-dependent, caveolin-dependent or other routes of entry, including lipid raft dependant entry (Smith & Helenius, 2004). During endocytosis, the binding to cell-surface receptor/receptors is followed by a subsequent exposure to acidic environment. The acidic pH triggers a series of conformational reorganizations in the virus ultimately leading to fusion of the viral and cellular membranes. The broad host-range among the different alphaviruses suggests the use of a common or possibly the usage of a variety of receptor molecules (Byrnes & Griffin, 1998, Helenius et al., 1978, Oldstone et al., 1980, Wang et al., 1992). Alphaviruses have been shown to bind to the major histocompability complex (MHC), laminin and heparan sulphate molecules but the specific receptor has not been conclusively defined. After receptor binding the virus is delivered to the endosomes via the entry pathway of clathrin coated pits (Helenius & Marsh, 1982, Simons et al., 1982, Smith & Helenius, 2004). However, a model where the virus fuses at the PM has also been proposed (Fan & Sefton, 1978, Paredes et al., 2004). The low pH environment during the endocytic pathway triggers conformational changes in the viral proteins leading to fusion peptide exposure and interaction with the target membrane. A subsequent structural reorganization, via E1 homotrimerization, ultimately leads to membrane merger and NC release into the cytoplasm. Disintegration of the NC to release the viral genome is fast and may involve interaction with ribosomes but this mechanism is not fully understood (Greber et al., 1994, Singh & Helenius, 1992, Wengler, 1984).

1.3.2 Replication

Replication of SFV is highly efficient and takes place in the host cell cytoplasm (Strauss & Strauss, 1994). Following fusion of the viral and endosomal membranes is release of the NC into the cytoplasm. The NC dissociates releasing the 42S (11.5 kb) positively stranded RNA genome. Once accessible to the host-cell replication machinery, the nonstructural proteins can be translated. The nonstructural proteins (nsP1-nsP4) are directly translated from the first two-thirds of the genomic RNA as a precursor polyprotein that after processing forms a replication complex called either a replicon or replicase. Viral replication and transcription has been shown to be associated with endosome-derived vesicles known as cytopathic vacuoles type I (CPV I) (Acheson & Tamm, 1967, Grimley et al., 1968, Kujala et al., 2001, Peranen & Kaariainen, 1991). The replication complex transcribes a complementary negative strand RNA later involved in the replication of the full length positive stranded 42S RNA, as well as a subgenomic 26S RNA (4.1 kb). The 26S RNA, corresponding to the last one-third of the genomic RNA, acts as a template for the synthesis of the structural proteins. Newly synthesized 42S viral RNA becomes encapsidated by the C protein forming NC's, which is involved in the budding of new virions at the PM.

1.3.3 Assembly and budding

Assembly and budding of alphavirus has been studied extensively and reviewed in many articles (Garoff et al., 1998, Garoff et al., 2004, Strauss et al., 1995). Release of the capsid protein into the cytoplasm exposes a signal sequence in the p62 protein guiding it to the endoplasmatic reticulum (ER). After insertion into the ER the polyprotein is processed generating the E1, E2, E3 and the small 6K protein, as described earlier. Within the ER, E1 associates non-covalently with p62 into dimers that subsequently oligomerizes into heterotrimers before reaching the PM (Barth et al., 1995, Ziemiecki & Garoff, 1978, Ziemiecki et al., 1980). The p62 protein may function as a scaffold protein, both guiding correct E1 folding and protecting it from premature fusion with internal cellular membranes. A crucial step in the maturation process of the virus is the p62 cleavage which primes the acid susceptibility. The surface proteins of many enveloped viruses are often synthesized as inactive precursor proteins that are proteolytically primed during maturation to achieve full activity. This is to protect the virus particles from premature activation that correct activation can occur during the infection cycle. The function of the 6K protein in assembly and budding is not fully understood but it has been suggested to play a role late in the assembly pathway (Loewy et al., 1995, Lusa et al., 1991, McInerney et al., 2004).

In the current budding model, capsid proteins encapsidate newly synthesized viral 42S RNA into intracellular NC's. During budding the NC's impose their icosahedral symmetry by guiding the preassembled spikes to organize on the PM with the same symmetry as the underlying NC template. These NC-spike interactions are believed to be the driving force for the assembly and pinching-off new virus particles (Garoff et al., 2004, Helenius & Kartenbeck, 1980, Simons & Garoff, 1980). An alternative model where the spike proteins guide particle assembly has also been proposed (Forsell et al., 1995, Forsell et al., 2000). In these studies intact virus particles with correct organization were released although it was found that N-terminal deletions in the C protein prevented the cytoplasmic assembly of NC's. This suggests a model where the viral glycoproteins, probably arranged as spikes, organize the NC assembly and drives budding at the PM. Synthesis and assembly of the viral glycoproteins has been associated with tubular structures, with the glycoproteins on the inside and NC's at the exterior, described as cytopathic vacuoles type II (CPV II) (Acheson & Tamm, 1967, Griffiths et al., 1989, Griffiths & Gruenberg, 1991). The exact function of these cytoplasmic structures are not known but are assumed to be involved in virus assembly.

1.3.4 Extracellular phase

The alphavirus, also known as arbovirus (from arthropod-borne) group A, has a wide geographic distribution. Members of the alphavirus family are almost exclusively transmitted by mosquitoes infecting vertebrate hosts such as rodents and birds. The arthropod vectors acquire the viral infection by biting a viremic host. Alphaviruses can replicate in the vector's tissues and subsequently be transmitted through the salivary secrection into vertebrate hosts. The ability to infect and replicate in both vertebrate and

arthropod vector cells is an essential quality of alphaviruses. In most cases the virus is maintained in the primary host and is not further transmitted to humans.

1.4 VIRUS FUSION

Apart from being a protective shield during the extracellular phase the function of the envelope proteins is also to take an active part in particle disintegration. Enveloped viruses rely on fusion with the PM or internal membranes to deliver their genome into the proper cell compartment for propagation. Virus fusion processes in membrane-containing viruses such as retrovirus, orthomyxovirus, alphavirus and flavivirus have been intensively studied and reviewed in many articles (Dimitrov, 2004, Kielian, 1995, Kielian & Rey, 2006, Skehel & Wiley, 2000, Smith & Helenius, 2004, Zaitseva et al., 2005). Virus membrane fusion is mediated by the envelope proteins and can be classified according to their characteristics and the mechanistic pathway during the fusion step. Release of the accumulated energy locked in the locked in the structure, promoting the membrane fusion and particle disruption, is triggered by various means among different viruses.

The proteins active in membrane fusion have been divided into class I (type 1) and class II (type 2) fusion proteins. The fusion mechanism of class I fusion proteins, exemplified by the hemagglutinin protein 2 (HA2) of the Influenza virus, is currently better understood. Our knowledge about the class II fusion mechanism, as exemplified by the E1 protein of alphavirus, has progressed rapidly during the last several years, partially as the result of new structural information. The atomic resolution structure of both the neutral pH sE1 and the acid triggered sE1 homotrimer has been solved. They show very similar structure to the E proteins of TBE virus and suggest a similar class II fusion mechanism (Bressanelli et al., 2004, Gibbons et al., 2004b, Modis et al., 2004, Zaitseva et al., 2005).

The most distinct feature of the class I fusion protein, as exemplified by the HIV-1, Influenza or Ebola, is the refolding of the HA2 into a long α-helical trimer with the N-terminal fusion epitope exposed for target membrane interaction. The viral and host-cell membranes are subsequently brought in close proximity by a jack-knife-like refolding of the trimeric spike. This refolding positions the TM and fusion peptide at the same end of the HA2 molecule. Typical for the class II fusion proteins, unlike class I, is that their tertiary structures are mainly composed β-sheets essentially lacking helical motifs in the external part of the glycoproteins. The sequence homology of the respective fusion peptides between members in the class I and II is very low. In the native virus particle, the class II fusion proteins have been proposed to lie almost horizontally while they are vertically positioned along the viral membrane in the class I case. The fusion peptide in class I proteins is located at the N-terminus and buried in the trimer interface while in the class II fusion proteins it is internal and located at the end of the rod-like molecule. In this orientation the E1 protein becomes shielded by dimeric interactions with the companion E2 protein. Furthermore, the class I fusion

proteins do not have any requirements for cholesterol or target membrane composition. These characteristically significant differences suggest that the two types of fusion proteins would utilize two different fusion mechanisms.

1.4.1 Class I fusion mechanism

The structure and function of the fusion proteins in class I is exemplified by the HA2 of the influenza virus (Skehel & Wiley, 2000, Weissenhorn et al., 1999, Wiley & Skehel, 1987). During the Influenza virus maturation the precursor protein HA0 is proteolytically cleaved by host proteases into HA1 and HA2, where the former carries the receptor recognition domain and the later the fusion activity. Both proteins are anchored in the viral membrane, covalently linked to each other by disulfide bonds and form vertically oriented HA1-HA2 heterotrimers. Fusion activation is triggered by an acidic environment resulting in weakening of the subunit interaction. The receptor bound HA1 folds back, making room for the fusion peptide to relocate and interact with the target membrane. The neutral pH conformation of HA2 contains two anti-parallel α-helices separated by a loop (Wilson et al., 1981). Upon acid activation the fusion peptide, *i.e.* the N-terminus of the shorter of the previously mentioned α-helices, relocates from a hidden pocket, near the base of the spike, to position where it becomes exposed for membrane incorporation (Bullough et al., 1994). This almost 100 Å relocation of the fusion peptide has its origin in a refolding of a inter-helical loop resulting in an extended α-helix and part of a triple helix bundle. The next step is to bring the viral and host-cell membranes into close proximity so that lipid bilayer merging can take place. A part of the long α-helix closest to the membrane refolds into a reverse turn and aligns to the remaining α-helix anti-parallel against the first half. Thus, the α-helix folds back into a six helix bundle and brings the membrane anchored C-terminus closer to the host-cell bound fusion peptide. The exact nature of the remaining steps involved in membrane fusion are believed to involve bending of the membranes, formation of a fusion stalk/hemifusion stage, pore formation and finally the merging of the membranes.

1.4.2 Class II fusion mechanism

Our understanding of the class II fusion mechanism has improved significantly after the successful structure determination of both native and fusion activated E1 and E proteins of the alphavirus and flaviviruses, respectively (Bressanelli et al., 2004, Gibbons et al., 2004b, Lescar et al., 2001, Rey et al., 1995). The atomic resolution structure of the crystallized soluble ectodomains of both the E1 and E shows that they adopt very similar folding both in their native and fusion active conformations (**Fig. 4** and **5**). Based on their significant structural similarities, the fusion mechanisms of alphavirus and flavivirus are believed to be very similar and represent the class II mechanism. The rod-like E1 ectodomain is mainly composed of β-strands with connecting loops, and contains only a few short α-helices. The internal fusion peptide is located in a loop at the tip of domain II. At the other end of the 12 nm long rod-like molecule is the Ig-like domain III, carrying the C-terminal TM domain. The DIII is connected to domain I via

a flexible loop structure. Domain II is connected to the dimerization domain or domain I. In model fittings, E1 proteins are organized back-to-back and head-to-tail at the quasi 2-fold axes (**Fig. 2B**). In this fit domain III becomes aligned around the openings in the shell at the 2- and 5-fold axes and is in close contact to other E1 molecules from neighboring spikes. The obliquely positioned E1 molecule, with the domain III facing the 2- and 5-fold axes, hides the fusion loop under the bulky spike head (similarly as viewed in **Fig. 2A**, upper right). This modeling of the E1 molecule suggests that it constitutes most of the shell domain while the protruding and internal spike densities are mainly composed of the E2 protein.

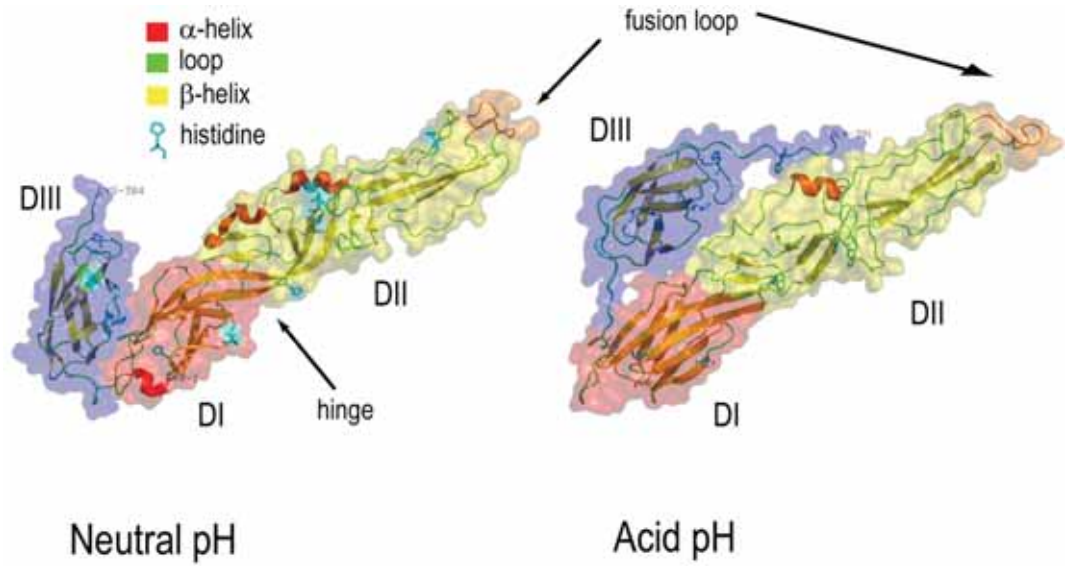

Figure 4. *Atomic resolution structures of neutral and acid pH treated E1 monomers.* Top views of the neutral (left) and acid (right) pH form of the atomic resolution structures of the soluble E1 ectodomains (PDB_ID:2ALA and 1RER, (Gibbons et al., 2004b, Roussel et al., 2006). The acid pH-induced E1 monomer was extracted from its crystallized homotrimeric form. A semi-transparent isosurface is over-layered highlighting the domains I (blue), II (red) and III (yellow), as well as the fusion loop (orange). α-helices (red), b-strands (yellow) and loops (green) secondary structures as well as the positions of the histidines and the C- and N-terminus is also shown. Positions of the histidines indicate regions in the E1 molecule sensitive to side-group protonisation at pH around 6.0.

One important prerequisite for the fusion-related protein reorganizations to take place under physiological pH conditions is the cleavage of the p62 protein. It has been shown that virus particles produced in furin deficient cells or virus with mutations in the cleavage site, like the SFVmSQL mutant, still undergo the essential structural changes and fuse with target membranes although at a much more acidic pH (Lobigs & Garoff, 1990, Salminen et al., 1992, Tubulekas & Liljestrom, 1998, Zhang et al., 2003). Exactly how such changes prevents normal fusion events is not known, but the covalently linked E3 protein must somehow prevent essential fusion related rearrangements and possibly the exposure of the fusion peptide. Several attempts to locate the E3 protein in the virus structure have been using cryo-EM structural analysis but its exact location has still not been definitively determined (Ferlenghi et al., 1998, Kenney et al., 1994, Paredes et al., 1998).

The fusion activation in alphavirus occurs via several identifiable intermediate steps such as the dissociation of E1 and E2 heterodimers, exposure of previously hidden antibody recognizable epitopes, changes in trypsin sensitivity and the formation of a stable E1 homotrimer (Kielian, 1995). It is believed that after dissociation of the tightly connected E1/E2 dimers, E1 proteins re-oligomerizes into homotrimers (Wahlberg et al., 1989, Wahlberg et al., 1992, Wahlberg & Garoff, 1992). Presumably prior to this E1 homotrimerization, a stretch of hydrophobic aa referred to as the fusion peptide or loop, located between aa Asp 79 and Asp 97 (Duffus et al., 1995, Garoff et al., 1980b, Levy-Mintz & Kielian, 1991). In intact virus particles, the E1 protein has been shown to be exposed only after acidic pH treatment (Hammar et al., 2003). It was shown in studies on pH treatment of soluble E1 ectodomains, in the presence of liposomes, that the fusion loop becomes inaccessible. This was observed as reduced binding of monoclonal antibodies (MAbs), earlier mapped to the fusion loop, and suggests a role for the fusion loop in target membrane interaction (Gibbons et al., 2004a). The exposure of the fusion loop and E1 homotrimerization is dependent on the lipid composition and the presence of cholesterol in the target membrane. The cholesterol dependence have been mapped to the Pro 226 in the E1 protein (Ahn et al., 2002, Chatterjee et al., 2000, Kielian & Helenius, 1984, Phalen & Kielian, 1991, Wilschut et al., 1995). Following membrane insertion a second stage of protein refolding of the viral proteins take place (Bron et al., 1993).

The structure of the fusion activated E1 homotrimer, similarly as in the neutral pH form, shows a rod-shaped molecule but now with domain I at the base and domain II carrying the fusion loop at the tip (**Fig. 4**). The Ig-like domain III, carrying the membrane anchored C-terminus, has been juxtaposed to extend along the sides of domain I and II covering the cleft between the subunits (**Fig. 5**). The homotrimer is held together essentially by interactions between β-sheet domains in domain I. Compared to the neutral pH structure there is a 15 degree bend of domain II at the interface between domain I and II, referred to as the hinge region. The fusion loops are not in close contact within the homotrimer and supposedly not the origin for the trimerization.

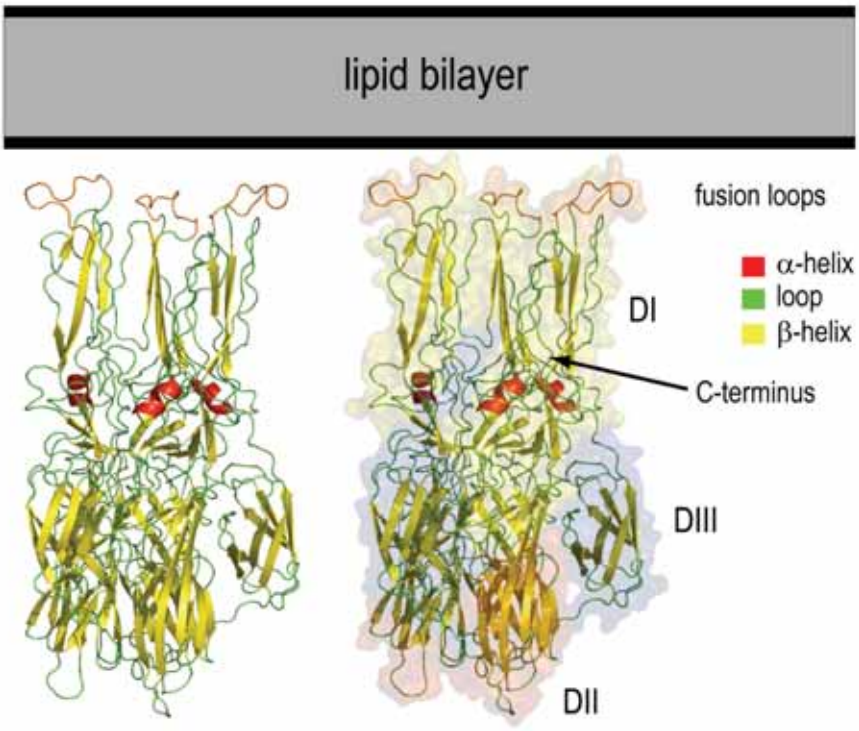

Figure 5. *Atomic resolution structure of acid induced E1 homotrimers.* Side views of the atomic resolution structure of acid pH induced E1 homotrimers (PDB_ID:1RER, (Gibbons et al., 2004b). A semi-transparent isosurface is over-layered highlighting the domains I (blue), II (red) and III (yellow), as well as the fusion loop (orange). α-helices (red), b-strands (yellow) and loops (green) secondary structures as well as the positions of the histidines and the C-terminus is also shown.The E1 homotrimer is positioned with the domain I with the fusion loops pointing to the fictitious target membrane. Note the relocation of the domain III from its original location to a position where it is aligned externally to domain I with the C-terminus also pointing towards the target membrane.

The E1 protein goes through a refolding process whereby domain III becomes folded back and positioned at the same end as the fusion loop. An extensive and cooperative refolding of the membrane inserted and vertically oriented E1 homotrimers, similarly as in class I fusion proteins, have been suggested to be the driving force to bring the host and viral membrane in close proximity. Based on inter-trimeric fusion loops contacts among the homotrimers in the crystal structure, and that these geometrically fit best as pentamers, it was suggested that pentamers of the homotrimers are involved in the actual membrane insertion and fusion (Gibbons et al., 2004b). Similar observations were made in the study preceding the crystal structure determination were acid pH treated and membrane inserted E1 displayed rings of five to six homotrimers (Gibbons et al., 2003). These observations lead to a model where the concerted action of a ring of five trimers creates a nipple or crater and deforms the target lipid layer. This would force the outer leaflet of the target membrane in close proximity to the deformed viral membrane. The bending of the membranes reaches a hemifusion intermediate stage where the outer leaflets becomes mixed as schematically shown in **Figure 6** (Gibbons et al., 2004b, Zaitseva et al., 2005). Finally a fusion pore is formed whereby the NC is released into the cytoplasm and replication can take place. However, the atomic resolution structure of the soluble E1 domain does not include the TM domain. In the native virus particle, the E1 molecule is connected to the limb domain followed by

anchoring to the viral membrane by the TM domain. Furthermore, the bulky E2 protein, located inside the spike, is likely a major steric hinderance for any central movements that would be the most obvious movement for homotrimerization. Therefore, it is challenging to mechanistically understand how the E1 homotrimers form and how breaking the virus symmetry would bring the target and viral membranes into close contact.

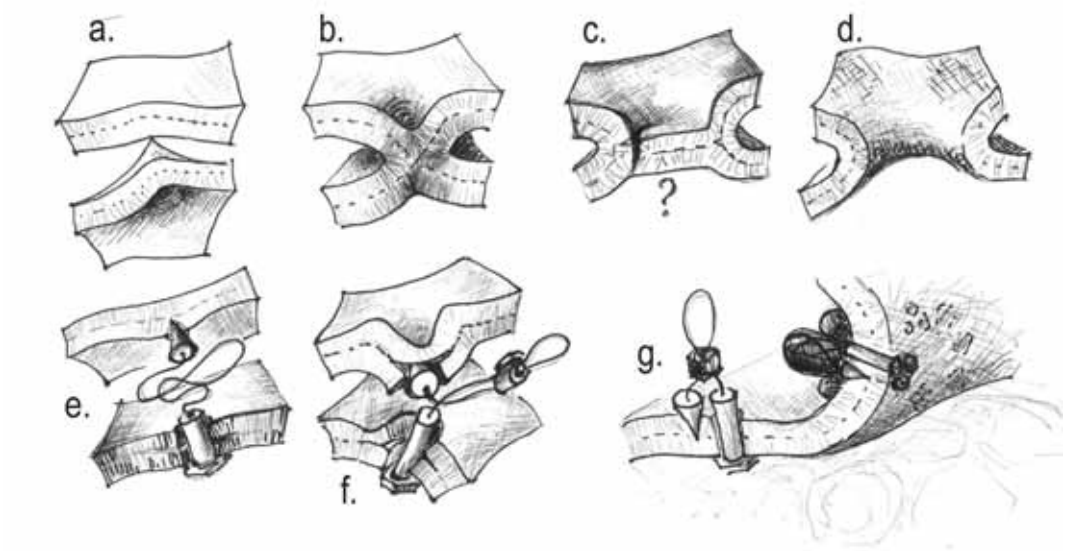

Figure 6. *Proposed model for the membrane fusion process.* Lipid bilayer membranes in contact by a local protrusion that penetrates the polar surface of the target and disturbs its hydrophobic interior phase (a). This may result in a stalk (b), or possibly a hemifusion (c) intermediate configuration, before formation of a pore and merging of the two membranes into a confluent layer (d). Viral fusion proteins enhance this process, by providing a fusion peptide (here depicted as a cone) and a trap, loaded for membrane capture (e), close encounter (f) and membrane fusion (g). During the process the fusion protein refolds in a series of intermediates that may include different levels of oligomerization. (From Hammar et al., 2004 and reprinted with permission from the publisher).

1.5 VIRUS INACTIVATION

1.5.1 Enveloped virus inactivation

Although virus inactivation methods often are well established, there are many factors that influence the inactivation efficiency (Sofer, 2002-2003). The method of choice depends largely on the type of virus to inactivate particularly enveloped or non-enveloped viruses. Various virus inactivation methods such as pH, heat, solvents, detergents, chemical treatment and UV irradiations have been applied successfully. The presence of contaminants, *i.e.* the purity of the virus, will also affect the inactivation efficiency. For the inactivation of enveloped viruses there is a natural low resistance to any physicochemical treatment due to the relatively delicate membrane. Heat, pH, detergent/solvent and various chemical treatments have often been used to inactivate enveloped viruses. The function of detergent likely has a dissolving effect on the envelope of the virus. For heat inactivation, temperatures above 60 °C are commonly used. Moreover, the moisture content also has an affect. Inactivation by environmental pH below 5 has been used and as the pH gets lower, the efficiency of inactivation

increases. Chemical inactivation often includes various cross-linking agents such as aldehydes. Formaldehyde (FA) is commonly used as a disinfectant in vaccine production. There are a wide range of methods to inactivate viral pathogens and the chosen method depends largely on the purpose. To preserve the particle morphology a more gentle approach is needed. Detailed studies of the structural effect on the virus after FA inactivation have so far not been conducted. Methods such as heat and detergent inactivation, although efficient in reducing the virus infectivity, would certainly be destructive to the virus structure.

1.5.2 Formaldehyde chemistry

Formaldehyde is a gas that readily dissolves in water, and solutions of 37-40 % are commercially known as formalin. Formaldehyde quickly dissolves in aqueous solutions and recombines into its reactive form methylene glycol/hydrate (OH-CH2-OH). The reactive methylene hydrate form can undergo polymerization in aqueous solutions into insoluble paraformaldehyde (PFA), a reaction that is inhibited by the addition of methanol. Depolymerization of shorter polymers occurs almost instantly in neutral pH buffers and is catalyzed by the presence of hydroxide ions and heating to 60 °C (Kiernan, 2000). FA reacts preferentially with charged primary amines (N-terminus and the side chain lysine residues in peptides and proteins) but also with other weaker nucleophilic groups such as hydroxyls and thiols. Because such a wide range of reactions are possible, complete characterization of FA modifications in proteins has not fully been accomplished. In the initial reaction of FA, highly reactive hydroxymethyls combines preferentially with uncharged amino groups, which in a second reaction with suitably spaced nucleophiles. The final product of this pair of reactions is a stable, covalent methylene bridge. These methylene bridges, or cross-links, are believed to be the most important modification caused by FA in proteins (Metz et al., 2004). The initial reaction, in particular with primary amines and thiol groups, is fast while formation of the methylene bridges is much slower. Cross-linking occur not only between reactive side chains, within the protein, but also to the amides of the peptide chain and are the origin for the fixative effect. However, as mentioned above, the exact effect of FA on a protein's secondary, tertiary or quarternary configuration is not fully understood (Puchtler & Meloan, 1985). It has been shown that FA does not change denaturation transitions, showing that the FA treated protein is not in a completely "locked" or fixed conformation. Moreover, infrared spectroscopy shows that there is no indication of changes in protein secondary structures (Mason & O'Leary, 1991). The secondary structure of a protein, largely determined by its primary sequence, dictates to high degree the overall folding of the protein. Since the reactivity of FA towards specific aa is dependent on factors such as protein configurations, different proteins will be modified differently.

1.5.3 Applications using formaldehyde

The use of FA as a disinfectant can be traced back to the end of the 19th century (Puchtler & Meloan, 1985). The fixative feature of FA for tissue preparations are

usually ascribed to F. Blum in 1893 and have ever since been frequently used in histology and pathology, despite its known toxic effects. Osmium tetroxide was used as the only satisfactory fixative before the introduction of FA, but its toxicity and other negative features made aldehyde fixation more popular. Nowadays, aldehydes are one of the most commonly used fixatives in structural studies of biological specimens where they serve to stabilize the fine structural details of cells and tissues prior to microscopy examination. Some aldehyde fixations includes a mixture of both FA and glutaraldehyde and are referred to as Karnosky's fixative (Karnovsky, 1965). The smaller molecule of FA enables rapid tissue penetration that initiates the structural stabilization while the glutaraldehyde is involved in the more thorough cross-linking since it can span greater distances. The lower tendency for FA to form longer polymers reduces the risk of sample aggregation when applied to single molecular objects.

Formaldehyde has also been used for decades as inactivating agent in virus vaccines and became well known during the introduction of the polio vaccine by J. Salk in the 1950's. Nowadays, there are several other physicochemical treatments for virus inactivation during vaccine development, including the use of urea, heat, pasteurization, detergent, solvent/detergent combinations, UV irradiation and psoralen treatments. The aim is to get a vaccine with completely abrogated infectivity but with well preserved antigenicity and immunogenicety which will effectively trigger a protective immunity in the host. The continuous use of FA probably reflects that it has a minor effect on the virus structure.

2 AIMS OF THE PRESENT STUDY

This thesis is focused on the class II viral fusion mechanism, as it occurs in SFV. The aim is to reveal molecular alterations within the SFV particle, preceding fusion. Therefore, the structure of the SFV has been determined and fusion related molecular reorganizations studied *in vitro* using acid challenged virions.

The work is presented as four separate papers with additional observations, covering details of the structural dynamics triggered by experimental acidification of the SFV virion. Specifically, the work has been focused on the following aspects:

- identification of functional epitopes exposed in a pH-dependent manner (*paper I* and unpublished data)
- rearrangements of the spike glycoproteins and domains close to the membrane (*paper II* and unpublished data)
- prefusion rearrangements of assigned domains in the external spike structure (*manuscript III*)
- effect of formaldehyde treatment on SFV morphology, infectivity and epitope preservation (*manuscript IV*)

3 COMMENTS ON METHODOLOGY

Detailed descriptions of the various methods can be found in the individual articles. Below are brief descriptions of the most commonly used methods.

3.1 VIRUS PRODUCTION

Sub-confluent monolayers of BHK cells were infected with SFV, clone pSFV4 (Liljestrom & Garoff, 1991), at multiplicity of infection equal to 10. After 18 hour incubation, the cell supernatant was cleared of cell debris and the virus collected as a pellet by prolonged centrifugation. The virus pellet was dissolved in TNM (50 mM Tris-buffer, 50 mM NaCl and 10 mM $MgCl_2$) buffer, pH 7.3, and subsequently purified by centrifugation to equilibrium in a potassium tartrate gradient. After fractionation the virus-containing fractions were pooled, diluted in TNM buffer, and centrifuged to form a virus pellet that finally was dissolved in TNM buffer. The virus was diluted and stored at a concentration of approximately 10 mg/ml (the virus concentration was estimated from light absorbance, where a value of A_{260} = 0.8 corresponds to a virus concentration of 0.1 mg/ml), which is equivalent to $9x10^{12}$ plaque forming units per milliliter (PFU/ml). All subsequent experiments were performed on freshly produced virus stored at 4 °C.

3.2 ANTIBODY PRODUCTION AND PURIFICATION

3.2.1 Hybridoma cell growth

All MAb expressing mouse hybridoma cell lines were a kind gift from Professor A. Salmi (Department of Virology, University of Turku). Hybridoma cell stocks, expressing the various MAbs used in the study, were thawed and cultivated and new cell stocks prepared to secure the future supply of the different MAbs. Initially the cells were grown in National Cancer Institute tissue culture (NCTC) supplemented Dulbecco modified Eagle's medium (DMEM) thereafter transferred into supplemented Roswell Park Memorial Institute medium (RPMI) and subsequently expanded. When adequate cell density was reached, the cells were transferred and finally grown in roller bottles. After approximately 5 days of incubation the cell supernatants were filtered and stored at -20 °C until further use.

3.2.2 Antibody purification

Hybridoma cell supernatants were pH adjusted using 10x PBS (Phosphate-buffered saline) and cleared of cell debris before purification. The cleared cell supernatant was applied to a Protein-A column (GE Healthcare Bio-Sciences) using the Ettan liquid chromatography system (GE Healthcare Bio-Sciences). The Protein-A molecule binds to the crystalizable fragment (fc) of the antibody with high affinity. After washing, the MAb was dissociated using a low pH buffer. To prevent protein denaturation, due to the exposure to the acid pH, fractionation was done into tubes containing a pre-titrated volume of PBS, pH 7.4. The MAbs were further concentrated and buffer exchanged using a Microsep™ microconcentrator (Pall Co.) into PBS buffer. The concentration of

the purified MAbs was estimated from light absorbance measurement (A_{280}=1 equal to 0.75 mg/ml). The purified MAbs were diluted to 2 mg/ml and stored at 4 °C in the presence of 0.05 % sodium azide. The general concentration of antibodies in the cell supernatants was on the order of 5 mg/l. One of the MAbs precipitated in the cold and was therefore kept in room temperature.

3.2.3 Antibody cleavage into fragments

To generate fabs, purified MAbs were initially dialyzed against a supplemented phosphate buffer. This was done to remove traces of the preservative included in the storage buffer. To activate the papain, which was used for the cleavage of the MAb, a reducing L-cystein buffer was added. Papain was added in a 100:1, antibody to papain molar ratio, and the cleavage mixture was incubated at 30 °C for 6 hours. The reaction was quenched with iodacetamide and analyzed on SDS-PAGE. The cleavage was very efficient under the conditions used and very little intact MAb remained uncleaved. Removal of the fc fragment was done by binding it to the Protein-A column. While immobilizing the fc fragments on the column the fab fragments was collected in the flow-through fractions.

3.3 PROTEIN CHARACTERIZATION

3.3.1 SDS-PAGE

The sodium dodecyl sulfate-polyacrylamide gel electrophoresis (SDS-PAGE) analysis was done using the Phast (GE Healthcare Bio-Sciences), miniVE (GE Healthcare Bio-Sciences) or mini-Protean® II (Bio-Rad Laboratories AB) gel systems and used according to the manufacturers recommendations. Virus samples were diluted in non-reducing or reducing sample buffer and heated at different temperatures (Laemmli, 1970). The visualization of the proteins in the gels was regularly done using Commassie Brilliant blue (CBB) or silver staining procedures.

3.3.2 Western blot

Subsequent to SDS-PAGE electrophoresis of the viral proteins, the proteins were transferred onto Polyvinylidene difluoride (PVDF) or nitrocellulose (NC) membranes under semi-dry conditions using the Mini Trans-Blot® (Bio-Rad Laboratories AB). Membranes containing the transferred proteins were blocked with Tween-20 and cut into appropriately sized strips before being incubated with the different MAbs. Following MAb incubation and necessary washing steps, the strips were incubated with a secondary antibody conjugated either with alkaline phoshphatase (AP) or horseradish peroxidase (HRP). The enhanced chemiluminescence (ECL) detection system, used for the peroxidase conjugated probes, was preferred because of its superior signal. The MAbs strong affinity to Protein-A suggested the use as reporter molecule in WB. Protein-A conjugated with peroxidase showed equal or slightly better signal than the fc-specific anti-mouse antibody in ECL detection. The Protein-A as reporter molecule enabled broader usage since it binds to antibodies raised in many different species. From the WB analysis, the different MAb-specific viral antigens could be assigned.

3.3.3 Pepscan analysis

The WB analysis assigned the specificity for the different MAbs. A more precise determination of their specific binding epitopes was determined using Pepscan analysis. Onto a cellulose membrane, the sequence of the viral proteins was synthesized in spots of 20 aa with 3 aa overlap. Similarly as in WB, the protein/peptide containing membranes were blocked and incubated with a MAb to be tested. The MAb, now bound to the respective spots of aa sequences, was transferred under semi-dry conditions onto a PVDF membrane. This enabled re-usage of the spot-containing cellulose membrane. Detection of the antibody on the PVDF membrane was done the same way as for WB. The location of the colored spots identified the linear sequences and hence the MAb specificity.

3.4 IDENTIFICATION OF EPITOPE ACCESSIBILITY IN THE SFV

3.4.1 ELISA

The enzyme-linked immunosorbent assay (ELISA) experiments were performed using Protein-A (GE Healthcare Bio-Sciences) affinity purified MAbs and gradient purified SFV particles. ELISA plates coated with SFV particles were blocked using bovine serum albumin (BSA). Tween-20 blocking showed a substantially lower signal and was likely an effect of dissolved virus particles. The purified MAbs, suspended in a pH buffer to be tested, were then introduced. Acid pH exposure prior to introducing the MAbs, in neutral pH solutions, was also tested and showed similar results. This indicates that the acid pH-induced molecular changes identified by the MAbs are not affected by the re-neutralization and thus show minor reversibility. Following MAb incubation and necessary washing steps, the wells were incubated with a goat anti-mouse antibody conjugated with HRP. Finally, HRP-specific color development using ortho-phenylenediamine dihydrochloride (OPD, Dako Sweden AB) was performed according to the manufacturer's recommendations. The reaction was quenched after reaching adequate color intensity, and the light absorbance was measured and treated as the level of MAb binding.

3.4.2 Biacore binding assay

Binding analyses using the surface plasmon resonance (SPR) technology were done using the BIAcore2000® system (Biacore Sweden). Gradient purified virus, Protein-A purified MAbs or fabs and commercial lectins were used. The sensor chips utilized had either a carboxymethyl coating (Sensor Chip CM5) or a layer of attached streptavidin (Sensor Chip SA). The immobilization of antibodies or lectins to the carboxylated dextran matrix of the CM5 chips was done using amine coupling chemistry. To immobilize SFV particles the streptavidin surface was conjugated with biotinylated Galanthus nivalis lectin (GNA) to which a high-mannose glyco-conjugate present in the E2 protein could be bound. Generally two different setups were used. Either the virus or the probe was immobilized whereby the analyte, suspended in different pH buffers, was injected. A second configuration was also used where the immobilized virus was

exposed to a pulse of low pH prior to being probed by the MAb suspended at neutral pH. These two approaches, similarly to the ELISA experiment, tested the reversibility of the conformational changes. The number of bound molecules per virus particle was determined. In these experiments the virus was bond to a lectin or antibody coated sensor surface (*i.e.* in a reversible way allowing regeneration) and the ligand injected until saturation. Experiments where the virus particles are immobilized prevent particle aggregation while in the experiments using pre-treatment, aggregation would accur during exposure to pH below 5.8. Immobilized virus could be regenerated with a detergent containing regeneration solution and the chip reused.

3.5 VIRUS INFECTIVITY

3.5.1 ELISA

SFV infectivity was analyzed using ELISA on the cell supernatants, collected 18 hours post-infection incubation, from cells infected with the virus specimen to be tested. In the ELISA, levels of the E2 proteins (and any uncleaved p62 protein) were detected using am antibody against the E2 protein (MAbE2v). The MAbE2v was selected as reporter antibody owing to its strong signal. Although, this antibody binds denatured proteins and can not differentiate between E2 proteins within virus particles or those free in the cell supernatant, its signal still gives a relative measure of the infectivity. This easy and relatively fast estimation of the virus infectivity was preferentially used during screening for optimal conditions of FA inactivation of virus particles.

3.5.2 Plaque assay

To confirm the virus infectivity as measured by ELISA, the more established plaque assay measuring the absolute virus titer was used. Confluent monolayers of BHK cells were infected with the virus sample. Before post-infection incubation, the cells were over-layered with an agar containing medium. The solidified agar prevents transmission of newly expressed virus particles. This restricted spread of virus, to the cells surrounding the initial infection site, eventually resulted in countable circular zones. The visibility of the plaques was enhanced by neutral red staining. Serial dilutions of the virus sample were tested and corresponding plaques counted. The infectivity expressed as number of plaque forming units per millimeter (PFU/ml) was calculated according to PFU/ml = number of plaques / dilution x volume.

3.6 VIRUS INACTIVATION

Gradient purified SFV particles, stored in TNM buffer, were dialyzed against PBS, pH 7.3, prior to FA inactivation. This was done to remove any traces of the amine containing Tris buffer that otherwise would interfere with the aldehyde reaction. The dialyzed virus was further diluted to give a final virus concentration of approximately 0.5 mg/ml. Several factors were thought to be important for the efficiency of the FA reaction: pH, FA concentration, temperature and time. The pH was kept at 7.3 and was not varied while the other variables were changed. The virus was treated with FA either at 4 °C or 20 °C by the addition of different volumes of 0.2 % FA (GE Healthcare Bio-

Sciences) to give the desired final concentration. A final FA concentration of 0.01 % corresponds to a molar ratio of roughly 350 000 FA molecules per virus particle.

3.7 CELL-CELL FUSION ASSAY

Confluent monolayers of BHK cells, grown on cover slips (18x18 mm), were infected with the dilution series of the virus specimen and necessary controls were included. The virus specimens were diluted in supplemented Eagle's minimal essential medium (EMEM). After a short exposure to a low pH buffer at 20 °C, the cells were further incubated at 37 °C in complete BHK-medium. The cells were fixed in pure methanol at -20 °C followed by a methylene blue fixation. Images of representative areas were recorded using a Leica ASM DW microscope (Leica Microsystems AB). The images were analyzed according to the number of nuclei relative to the number of cells. The extent of cell-cell fusion was calculated based on the formula Fusion = $1 - N_{cells} / N_{nucleus} \times 100$, where 100 represents complete cell-cell fusion.

3.8 VIRUS MORPHOLOGY ANALYSIS

3.8.1 Negative stain EM.

400 mesh copper grids covered with a thin carbon film were glow discharged making them hydrophilic. The virus specimen, diluted to approximately 0.1 mg/ml, was applied onto the grids and the excess solution was blotted off. The grids were washed with water before negatively stained for 10 s using 2 % uranyl acetate.

3.8.2 Electron cryo-microscopy (cryo-EM).

Three microlitres of gradient purified virus of adequate concentration was applied to holey carbon grids. The excess was blotted off before plunge freezing in liquid ethane. After the vitrification, the grids were transferred and stored in liquid nitrogen until further analyzed. During data collection, the grids were transferred into a cryo holder and inserted into the microscope while maintaining liquid nitrogen temperatures. The micrographs were recorded under low dose conditions onto Kodak SO163 (Eastman Kodak, Rochester, NY) films using a Philips CM120 or a JEOL SF3100 microscope.

3.8.3 Image analysis.

Micrographs taken at nominal magnifications of x28.000 or x40.000 and multiple defocus levels were digitized using a Zeiss SCAI scanner with 14 μm step resolution and 8 bits grayscale. Initial particle selection and data processing were done using the RobEM software (http://cryoem.ucsd.edu). The particle centers and orientations were determined, and iteratively refined against a successively improved 3D virus density map, using the model based polar Fourier transform (PFT) software package (Baker & Cheng, 1996), http://cryoem.ucsd.edu). When a stable reconstruction had been achieved, successively higher frequency information was included in the new cycles of refinement. Particles included for the computation of new refined density maps were selected primarily based on their real space cross-correlation coefficients. A high and

low pass Fourier filter was utilized in the computation of the 3D density maps to suppress both the low and high frequency information. The low-pass filter was set to exclude any frequencies beyond the first zero of the phase contrast transfer function (CTF) so that there was no need to correct the reconstructions. All 3D visualizations were carried out using the IRIS Explorer software (The Numerical Algorithms Group Ltd, Downers Grove USA).

4 PRESENT STUDY

4.1 THE ANTIGENIC SURFACE OF SFV (PAPER I)

The SFV enters the cell by endocytosis wherein it is exposed to a low pH. The low pH is necessary to trigger the next step of infection, which is to release the genome into the cytoplasm after fusion with the endosomal membrane. The SFV was exposed to different pH to mimic that environment. The aim is to explore how different domains at the virus vary in response to the acid treatment, and in this paper, we focused on the acid induced variations in epitope exposure. This is done by real-time measurements based on a surface SPR technology. Monoclonal antibodies and lectins were used as probes. Basically two different setups where used: either having the virus or the probes immobilized onto the surface of the sensor. The probes or the virus, suspended at the pH to be tested, were then introduced in the flow. The regeneration of the sensor surface destroyed the virus, so that it was reversibly immobilized and replenished between the runs. This was accomplished by coating the sensor surface with an antibody or the lectin GNA. In the experiments where the virus was immobilized, both stoichiometry and kinetic measurements at different pH using fab fragments were analyzed. Irreversible changes in the virus structure were also analyzed in experiments introducing a low pH pulse in the flow over the immobilized virus before the MAb. In this setup, the MAb binding took place at neutral pH that the MAb itself was not affected by the pH environment. Using cryo-EM we analyzed the particle morphology within the pH range tested. WB and Pepscan analyses were used to characterize our set of MAbs with respect to target antigen and sequence of linear epitopes. These characterized molecular probes were subsequently used to identify the accessibility of biologically relevant epitopes in the virion.

4.1.1 Result and discussion

From WB and Pepscan analyses we could assign MAbs as probes for functional virus domains, such as the putative receptor binding region (MAbE2r), a sequence close to the high mannose site (MAbE2m), and a variable domain (MAbE2v), all within the E2 glycoprotein. In the E1 glycoprotein, the fusion peptide loop was recognized by the MAbE1f. The respective linear epitopes for the MAbs are summarized in **Figure 7**.

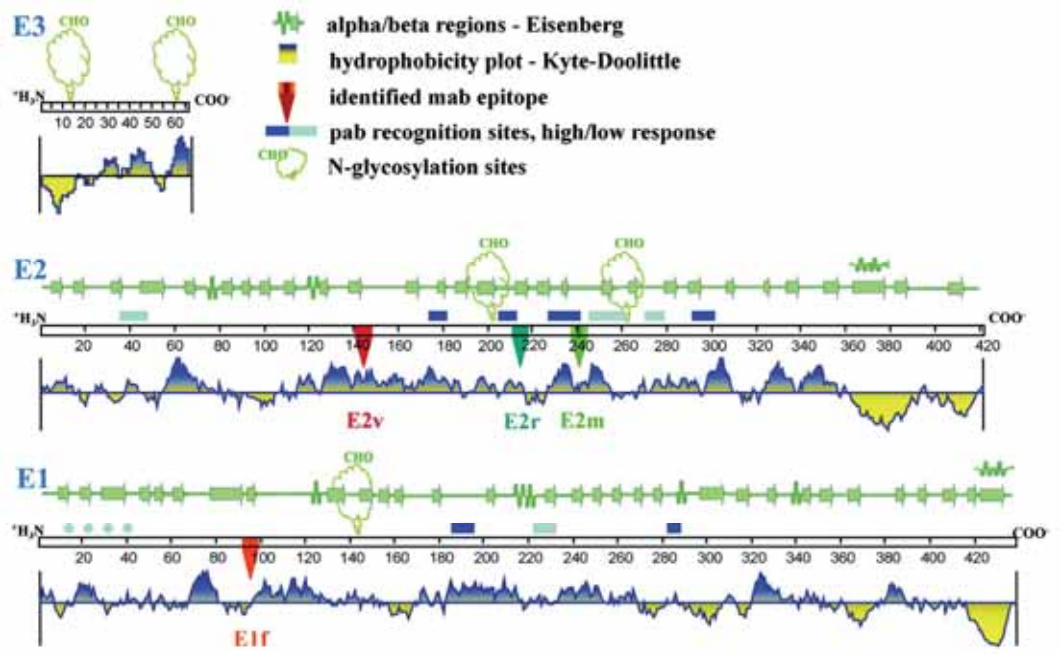

Figure 7. *Summary of the MAb specificity to the SFV glycoproteins.* Schematic representation of the Semliki Forest glyco-peptide sequences with secondary structure predictions, above a hydrophilicity-hydrophobicity plot. The positions of the Mab epitopes are indicated as well as the positions of the N-linked glycosylation sites. The blue bars above the sequence represent the found linear epitopes of the polyclonal sera.

The characterized MAbs, along with a conformation-specific, neutralizing MAb (MAbE1n) and various lectins were found to bind to the virus and *vice versa* in a pH dependent manner over a broad pH range (**Fig. 8**). As the Biacore studies reveal, the initial phase of acidification involves a transient exposure of the neutralizing epitope in the virus particle. Concurrent with the disappearance of the neutralizing epitope at pH conditions lower than pH 6.5, a set of masked sequences in the both E1 and E2 glycoproteins become exposed for external interaction. This includes the epitopes close to the receptor binding site at Thr211 to Asn218, a sequence close to the high-mannose sugar site at Asn 262 and an epitope at Thr1 42 His 146 in a variable region of the E2 sequence. Simultaneous with an increased virion diameter, the fusion loop at Lys 85 to Asp 97 becomes exposed with a pH optimum below 6.0. In this virus conformation, close to 80 fab fragments of MAbE1f (fabE1f) could bind per virion, corresponding to one ligand per spike. At neutral pH, only 15% of that binding was achieved. The fab fragment of the neutralizing MAb, fabE1n, showed an opposite binding profile with maximum at just below neutral pH and only 15 % of that at acid pH. In contrast to the antibodies, the lectin GNA, binding to the high-mannose glyco-conjugate in the E2, was less sensitive to pH variations. Furthermore, we could show that GNA reaches saturation levels at neutral pH with a one-to-one ratio to the target, *i.e.* three GNA molecules per spike. The molecular mass of GNA is 52 kDa which is close to the mass of a fab. Therefore, the lower stoichiometry of the fab E1f and E1n either reflects a restricted exposure or steric competition for binding at close sites.

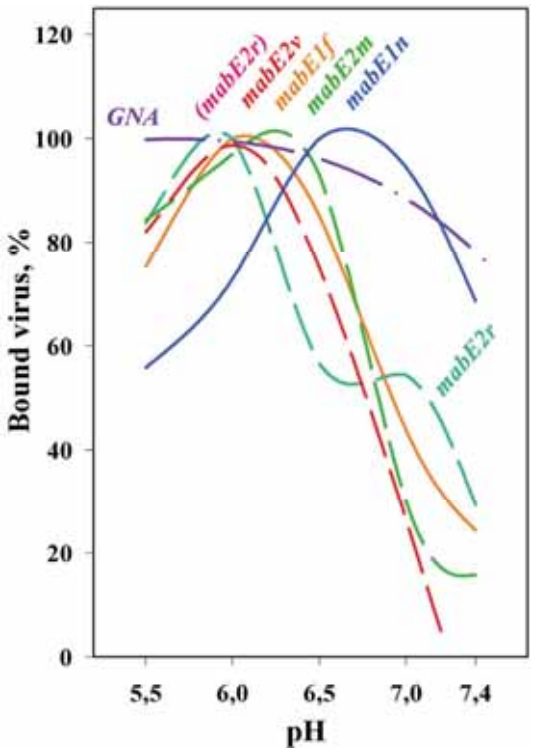

Figure 8. *pH-dependent binding of acid treated SFV particles to immobilized mAbs.* Overlay plot summarizing the pH-dependent binding of SFV to sensor surfaces coated with a series of MAbs and with results from the mannose-binding lectin from G. nivalis (GNA). The virus was incubated at the indicated pH and introduced in the flow over the sensor surfaces. Prior to analyze the usage of adequate virus concentrations were assessed i.e. to produce a concentration-dependent response. The results are presented as percent maximal binding with the used virus concentration.

Within the pH range analyzed we could show that the SFV particles behave as separate single particles down to pH 5.8 where they then appear as large aggregates (**Fig. 9**). The diameter of the particles increases continuously as the pH is lowered. From pH 7.4 to the most acidic pH examined by EM, pH 5.9, the size increases 13Å to a total diameter of 692Å. At pH 5.9 the particles display a relatively uniform size distribution which points to a homogeneous sample in a stable configuration.

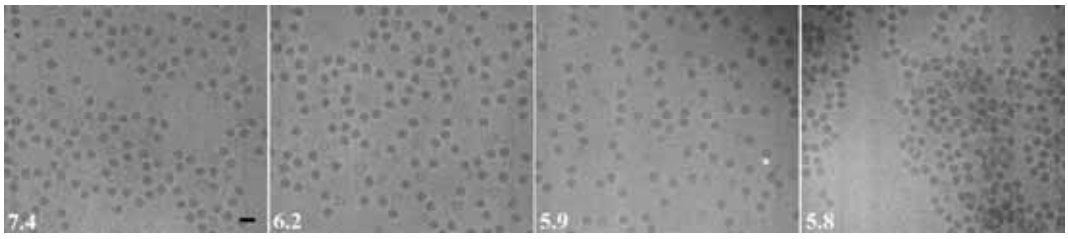

Figure 9. *Electron cryo-EM micrographs of SFV.* Gradient purified SFV virions was treated at the pH indicated for 1 min before plunge-frozen in liquid ethane. Micrographs were recorded at 28,000 nominal magnification at -3.0 µm defocus using a Philips CM-120 microscope. The bar represents 100 nm.

4.2 THE PRE-FUSOGENIC STATE OF SFV (PAPER II)

The acidic environment within the endosomes is known to trigger the alphavirus so that the fusion between the viral and host cell membranes can take place. In this study we wanted to visually identify the early molecular reorganizations within the SFV particle that lead to the fusion-active virus conformation. We exposed purified SFV particles

under carefully controlled conditions to different pH, searching for the lowest pH at which they still appear as separate single virus particles. This was done to allow for 3D reconstruction by single particle image analysis. Cryo-EM micrographs of gradient purified virions exposed to the different pH values were recorded and subsequently analyzed. From the reconstructed 3D density maps, we could identify several molecular reorganizations within the virus particle. The more pronounced details are seen in a comparison between the virus at pH 7.4 and 5.9. However, as discussed in *paper I*, this is a gradual process, with several distinct stages.

4.2.1 Result and discussion

An apparent increase in particle size after low pH exposure was observed. This follows the trend shown in *paper I*, with populations of particles of distinct and gradually increasing size. We observed a 2 % increase in the overall particle diameter as an effect of the acidification from pH 7.4 to 5.9 (**Fig. 10**). Particles exposed to pH 6.2, the reported threshold for fusion (Kielian et al., 1984, White & Helenius, 1980b, White et al., 1980), represent a stage of intermediate size increase. The gradual size expansion likely reflects transformations through a series if intermediate conformational stages.

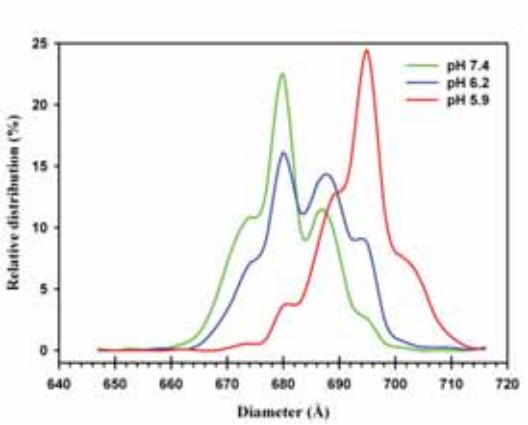

Figure 10. *Particle size distribution of pH treated SFV.* Size distribution of the SFV particles after exposure to pH 5.9, 6.2 an 7.4, as calculated from the images of orientation-refined virus particles from the cryo-EM micrographs. The curves represents bin averaging of number of particles within groups of 3 Å normalized to the total number of particles. The total number of particles in each sample was > 900.

During the structural analysis, we found that the particle expansion occurrs exclusively in the region above the lipid bilayer, where the E1 and E2 glycoproteins are confined into the shell and the spike-like protrusions (**Fig. 11**). Alterations in what was assigned to the limbs, the region connecting the glycoprotein spikes and the membrane, were observed contributing to the elevation of the shell domain. Other major protein rearrangements likely responsible for the elevation could be traced to reciprocal movements of the E1 and E2 glycoproteins relative to each other in the spike trimer. E1 modeling made it possible to suggest E1 and E2 density assignments to help in the further analysis. The observed movements not only affected the size of the virus but also affected the E1 shell, seen as an expansion of the holes located at the 2- and 5-fold axes (**Fig. 11**, compare the openings of the shell).

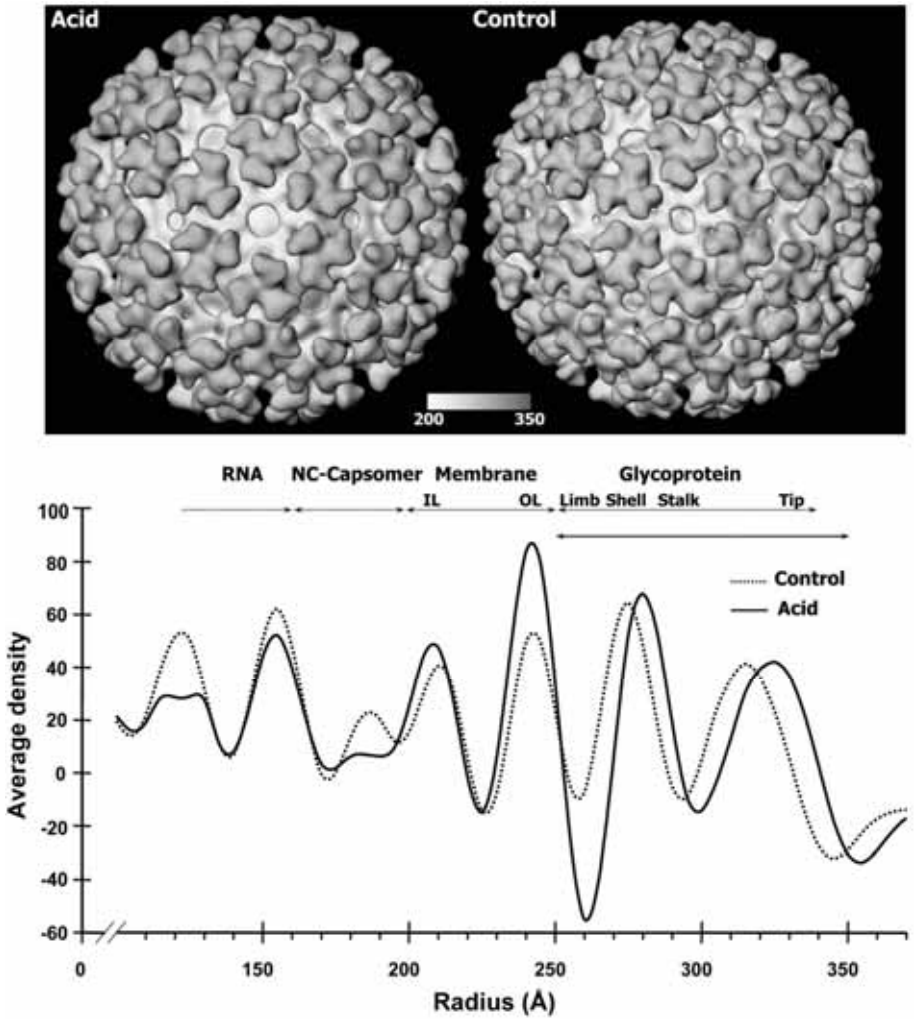

Figure 11. *Cryo-EM density maps of control and acid treated SFV.* SFV reconstruction of SFV exposed to pH 5.9 (acid) and 7.4 (control). Isosurface renderings of the acid (top left) and control (top right) 3D-reconstructions viewed along the 2-fold axis. Both structures contain 80 icosahedrally arranged characteristically tri-lobed projecting spikes. The spike bases are edged by the horizontal support known as the shell, which almost continuously connects the spikes apart from the holes seen at the 2- and 5-fold axes. Note the expansion of the holes in the structure of the acid treated SFV. Average radial density profile of the acid (solid line) and control (dotted) 3D-reconstructions showing the different layers of the virion (bottom). The different radial domains are indicated at the top of the graph. Most externally is the tip (head) of the spike followed by the stalk, shell, limb, OL (outer layer) and IL (inner layer). Interior of the particle comprises the NC with the C-terminus facing the inner lipid layer and the N-terminus in interaction with the viral positive ssRNA. Note the shift outward of the peaks corresponding solely to the E1 and E2 glycoproteins while the peaks corresponding to the lipid bilayer remain their radial position.

The shell expansion results in a larger surface area. However, the widening of the 2- and 5-fold holes occurs in an independent manner, pointing to specific molecular relocations in the surrounding structure. When comparing the control and acid structures, we observe compression and a slight bending of the E1 shell domain and an additional reshaping of the entire spike (**Fig. 12**, upper). The spike stalk becomes longer and the spike gains height by approximately 5Å. Modeling suggested that the E1 molecule projects obliquely from the shell, with domain III facing the 2- and 5-fold axes, toward the lower part of the spike head. In the acid treated virus, the corresponding density follows a steeper path (**Fig. 12**, lower).

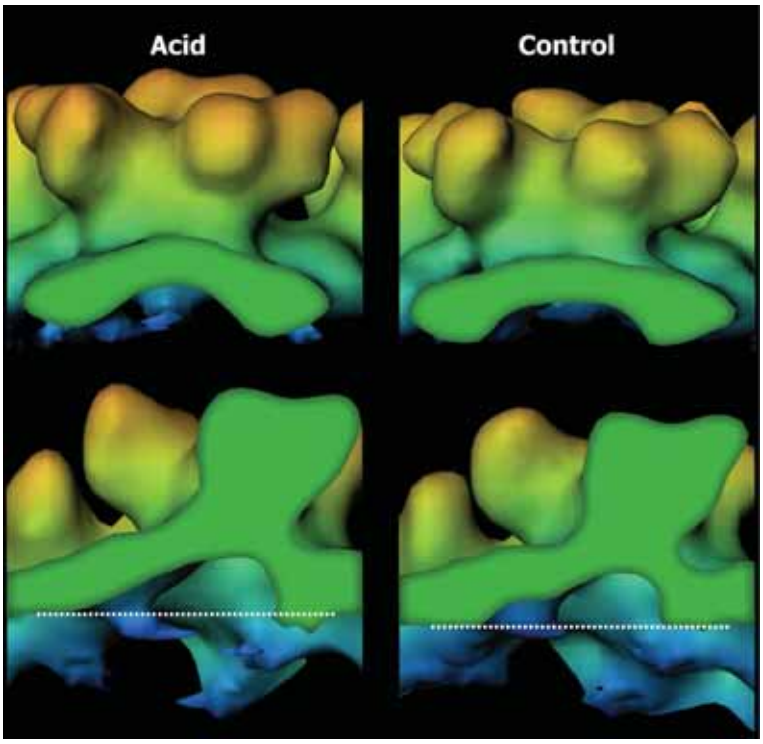

Figure 12. *Spike morphology of the control and acid treated SFV.* Isosurface representation of the 3-fold spike morphology extracted from the acid (left) and control (right) SFV reconstructions radially color coded. Side views of the spike cut and viewed along the quasi 2-fold axis (top panel) and cut along the direction of the proposed E1 location (bottom panel). Note the acid-induced compression of the shell region (top panel), the more upraised density (bottom panel) and the overall elevation of the whole spike.

A counter-clockwise twist of the assumed E1 density in the spike head occurs simultaneously with a clockwise movement of the (assumed) centrally located E2 density in the stalk region (**Fig. 13**). We speculate that these reciprocal movements would expose the fusion loop of the E1 molecule at the tip of the spike and promote interaction with the target membrane. These speculations are based on the observed binding of the antibody targeted to the fusion loop epitope at that pH, see *paper 1*. Because the resolution of the reconstructed density maps was not detailed enough to assign the separate contribution of E1 and E2 molecules in the bulky spike head, we focus in this paper on protein rearrangements close to the membrane domain of the envelope.

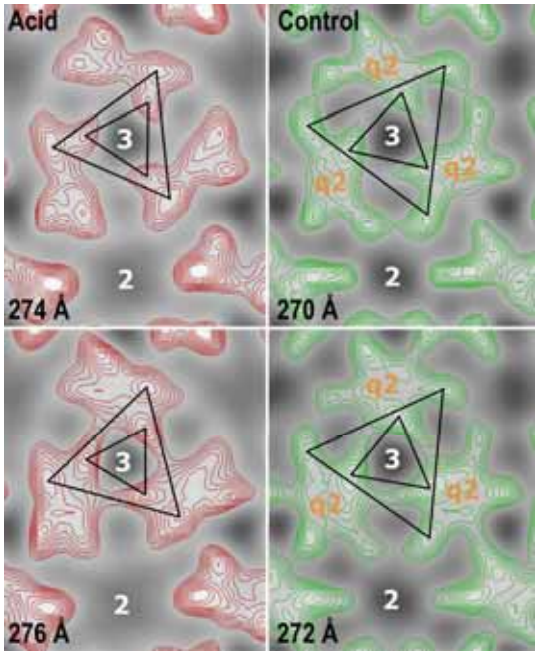

Figure 13. *Density distribution in the glycoprotein shell.* Density distribution in the glycoprotein shell around the 2-, 3-, and quasi 2-fold axes at defined radii of acid treated and control SFV reconstructions. The density peaks are emphasized by the red (acid) and green (control) contour lines for two pairs of roughly equivalent, consecutive radial sections (2 Å apart) in the middle of the shell region. The sections are compared 4 Å apart to compensate for the elevation of the glycoproteins in the acid treated virus. Density peaks around the 2-fold axis, connected to form the large triangle, is tentatively assigned to the domain III of the E1 protein. The more centrally located density of the 3-fold spike connected to form the smaller triangle is assigned to the E2 protein. As can be seen from the position of the triangles there is a reciprocal movement of the two proteins. As an effect of the acid pH the E1 protein tend to move counter-clockwise while the central E2 assigned density rotate clockwise.

An observation, although not that obvious, is the weakening of a density just below the membrane at the center of the hexameric and pentameric capsomers of the NC (**Fig. 14**, not included in the article). This is the region where the reported interaction of the sub-membrane tail of E2 and the capsid proteins occurs (Skoging & Liljestrom, 1998, Skoging et al., 1996). This interaction mediates the contact between the outer protein envelope and the internal NC. Loss of this density might be a result of an increased flexibility of the E2 sub-membrane tail and could lead to a destabilization of the envelope-nucleocapsid contact and also to enhanced mobility in the TM and limb domains. The nucleocapsid-E2-tail interaction is reported to be mainly based on the hydrophobic interactions of Tyr 399 in a hydrophobic pocket at the top of the capsid protein. Additionally there are several cysteines in the E2 tail and palmitoylation of these, likely to be involved in organizing the sub-membrane sequences correctly, are reported to be important for proper budding of the virus particles. We believe that this sub-membrane interaction is very important not only for stability reasons but also for its biological function both during assembly and membrane fusion.

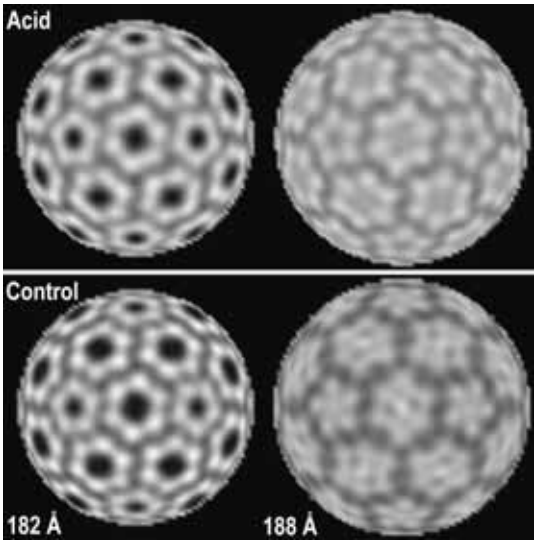

Figure 14. *Density distribution in the sub-membrane domain.* Radial cued density distributions in the sub-membrane region viewed along the two-fold axis. The 3D-reconstructions of the acid and control virus were cut at radii corresponding to the inner lipid layer and the capsid proteins. The strong densities represent the capsid monomers within the NC. Note the centrally located strong density at the 2- and 5-fold axes only seen in control virus at radius 188 Å. This density is not discerned in the acid treated virus.

4.3 THE DYNAMIC ENVELOPE OF SFV (PAPER III)

Paper III was an extension of *paper II* where improved cryo-EM 3D reconstructions of SFV at neutral and acid pH are presented. Thereby, the molecular reorganizations occurring upon acidification can be analyzed at higher resolution. The improved reconstructions were made possible mainly due to improved data collection using a field emission gun (FEG) electron microscope equipped with a helium cooling system. The lower temperature minimizes the specimen beam damage and the FEG emits a more coherent electron beam, ultimately leading to improved high-frequency information. Cryo-EM micrographs of gradient purified SFV particles exposed to pH 5.8 and 5.9 were collected using this microscope. The 3D density maps were reconstructed and analyzed by comparison to the neutral pH 7.4 structure. Based on E1 modeling, density assignments were made and the effect of acid pH treatment could be analyzed.

4.3.1 Result and discussion

pH-dependent morphology changes. Three-dimensional reconstructions of SFV exposed to pH values of 7.4, 5.9 and 5.8 were refined and computed to similar resolution. The reconstructions were analyzed for differences as a result of pH-dependent reorganization of the virus structure. The general particle morphology with its icosahedral symmetry of 80 tri-lobed spikes is essentially retained (**Fig. 15,** upper). However, and in congruence with earlier data (Haag et al., 2002) an apparent feature is the acid induced swelling. The increased diameter is evident by comparing the SFV structures in cross-section views and in one-dimensional (1D) density plots (**Fig. 15**, lower). The virus diameter gradually increases from 707 Å at pH 7.4 to approximately 727 Å at pH 5.8. As seen in a plot of averaged radial density, the thickness and radius of the lipid bilayers are retained, while the external protein layer has expanded.

Variations in the protein contacts are observed in the stalk and shell regions. The stalk region has become more elongated while the shell domain has been lifted outwards (away from the lipid bilayer) by about 7 Å in the structure determined at the most acidic pH. As a consequence, the openings at 2- and 5-fold axes in the shell layer are widened and the limbs became thinner and more elongated.

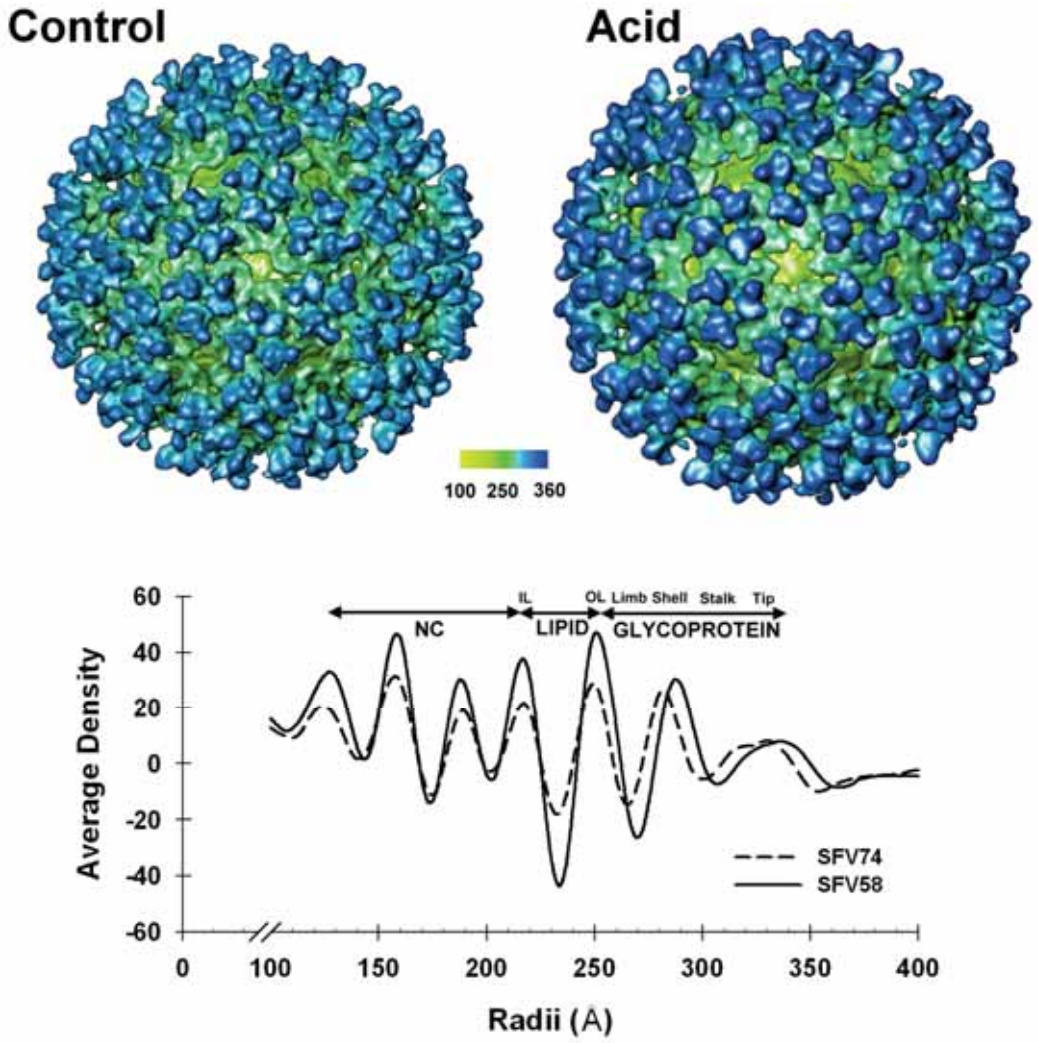

Figure 15. *Cryo-EM density maps of control and acid treated SFV.* Three-dimensional structures as reconstructed from cryo-EM micrographs of SFV particles pre-treated to pH 5.8 (acid) and 7.4 (control). The isosurface renderings are viewed along the 2-fold axis and represent 100 % mass and are radially color coded as indicated (top panel). The virus structure after pH treatment is observed swollen but still with a well preserved exterior with the 80 spikes icosahedrally in a T=4 symmetry arrangement. Note the expansion if the shell openings at the 2- and 5-fold axes in the acid treated structure. One-dimensional plot of the average density distribution showing the density peaks corresponding to the different layers of the virus as indicated (bottom). The particle size expansion is seen as a shift of the radial density peaks corresponding to the E1 and E2 glycoprotein layer.

Assigning reference domains in the SFV cryo-EM structure. Strong density centers seen in the cryo-EM reconstructions were denoted as density nodes. The density intensity is illustrated by a color scale, and contour lines representing increasing sigma levels. These nodes originate from stable sub-domains in the 3-D structure, among which should be candidates for prominent β-sheets or β-barrel domains. Most of these could be traced in the structures of the virus treated at different pH. Their interplay therefore

provides a means to follow pH dependent relocations in the structures. An assignment based on fitting known atomic models was done in an attempt to determine which parts of the 3D structure corresponds to the two glycoproteins. The atomic structure of sE1, determined from x-ray diffraction of crystallized E1 ectodomain dimers, is available in the protein databank (PDB_ID:2ALA, (Roussel et al., 2006). The atomic structure of a monomer was fit into our cryo-EM density maps of SFV at pH 7.4 based on manual fitting (**Fig. 16A**).

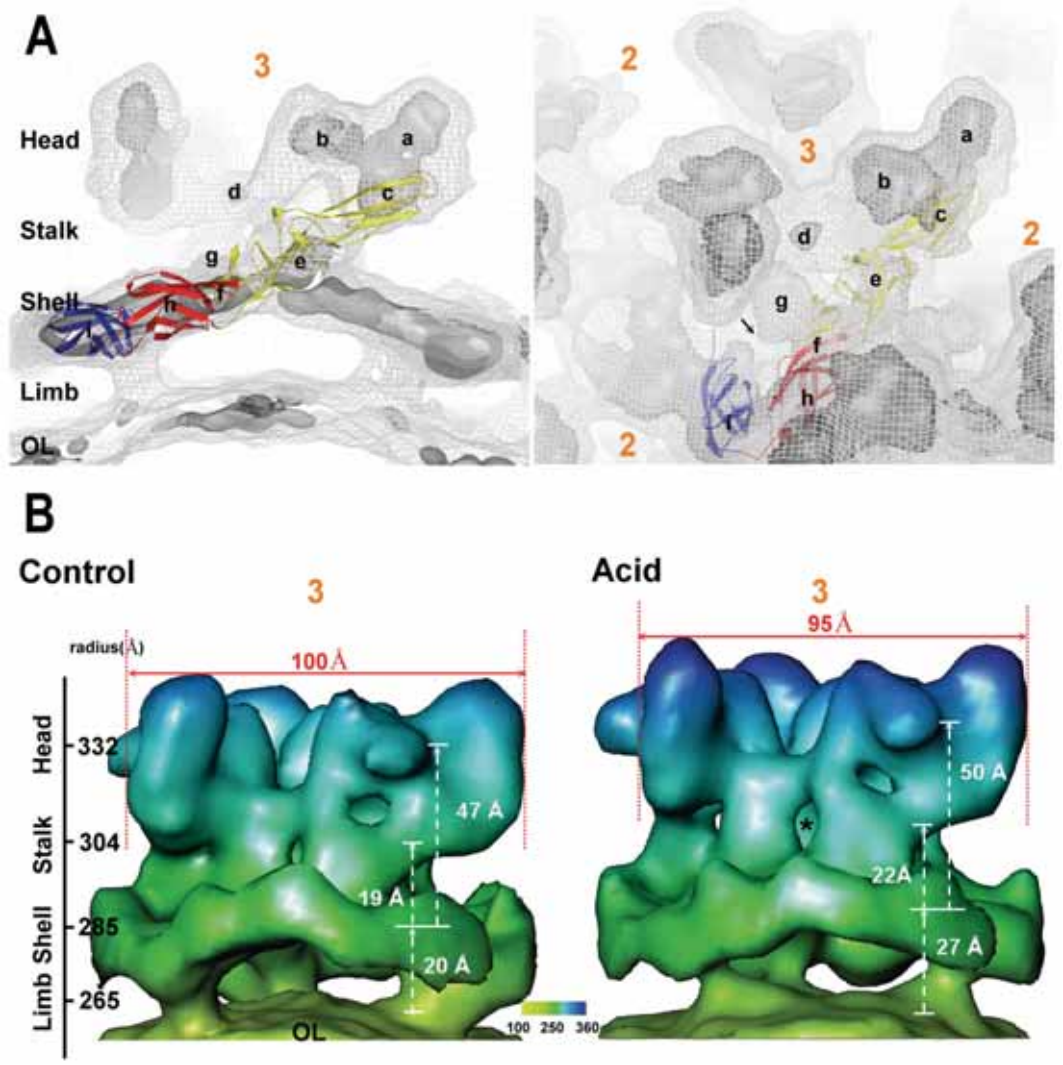

Figure 16 . *E1 model fitting and spike morphology of the control and acid treated SFV.* (A) Assignment of the respective density distribution in the control cryo-EM reconstruction from model fitting of the atomic resolution E1 structure. A side view as seen from the q2-fold (left) and a tilted view (right) showing the assignment of the density nodes. The 15 Å resolution cryo-EM reconstruction is rendered with an isomesh set to σ=1 and isosurface set to σ=3. The different domains of the E1 protein are color labeled and the different layers of the virus are denoted (O.L. = outer lipid layer). (B) Extracted 3-fold spikes from the control and acid pH reconstructions radially color coded. Note the discrepancies in spike morphology and the more upraised spike after acid treatment as pointed out by the measurements.

Our models places the E1 domains I and III in the shell region in close contact with other E1 molecules around the 2- and 5- fold axes, while domain II seems to best fit to a dimer-like interaction with the E1 of the neighbor spike at the quasi 2-fold axis. As a consequence of this fit, the domain II continues along the side of the stalk of the spike

and should contribute to the bottom of the spike head (**Fig. 16A**, left). The proposed fit of the 120 Å long E1 ectodomain structure suggests that the remaining density corresponding to the E2 protein is also an elongated molecule. It covers the E1 at the top of the spike tip and probably follows a relatively vertical path in the spike inside the E1 molecule. The E1-E2 dimeric contact in the head of the spike is complemented by contacts in the stalk region that hold the spike together. From examination of the E1 fit in the neutral structure, it is evident the domain III and domain I β-sheet structures fit into the density nodes denoted *i* and *h* (see **Fig. 16A**). Following the part of the 3D structure assigned to E1, there is a reasonable alignment of small nodes in the stalk region with the structure in the E1 molecule. However, there is a loss of congruence in the region where the E1 domain II enters into the bulky spike head. Nevertheless, with the density nodes corresponding to E1 and E2 proteins assigned, the interplay of the two molecules during prefusion rearrangements can be approached.

Relocations in the glycoprotein domain related to pH variation. The overall expansion of the glycoprotein layer generates slightly altered spike morphology and changes in the shell layer (**Fig. 16B**). The comparison of the control and acid pH structures of the density nodes within the spikes was done at different radius due to the overall expansion of the acid structure. Similar to earlier observations there is expansion of the shell openings at the 2- and 5-fold axes assumed to result mainly from domain III movements. As mentioned above, both the 5-fold and the 2-fold openings in the shell domain expand in the acid SFV structure. A close-up view of the 2-fold axis with modeled E1, indicates that domain III moves away from the center in the acid structure (**Fig. 17**). When the domain III is treated as a separate rigid body and individually fit into the lifted shell, a separation of the inter-connections of the domain III among the E1 molecules could be traced both laterally and vertically, along with a tilt upwards at the connection to the limb.

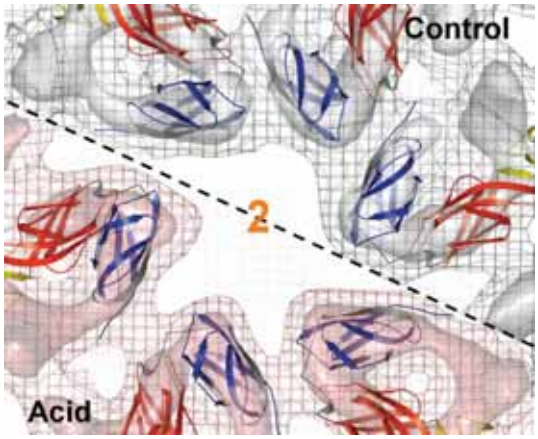

Figure 17. *Density distribution around the 2-fold axis.* Positions of domain I (red), II (yellow) and III (blue) of the model fitted E1 molecule in the shell layer around the 2-fold axis. The atomic resolution E1 structure was model fitted into the acid (top) and control (bottom) pH cryo-EM reconstruction. The isomesh (σ=1) and the isosurface (σ=3) renderings represents the density distribution of the cryo-EM density map viewed along the 2-fold axis. Noticeable is the more relaxed interactions of the densities corresponding to domain III, observed as a star-shaped hole 2-fold, in the acid treated structure.

Coincident with this movement, the limbs were dragged upwards, slimmed, and moved closer towards the 3- and q3- fold axes as observed in *paper II*. Nodes corresponding to domain I and II of the E1 protein move upwards as in a more vertically aligned molecule (**Fig. 18**). In the stalk region there is a counterclockwise movement of density nodes assigned to the E2 protein concomitant to a clockwise movement of the E1 protein. Consequently, the reciprocal movements of the E1 and E2 proteins are part of a process whereby the two proteins ultimately would dissociate. Moreover, model fitting of the domains I and II individually, allowing the hinge region between domain I and II to be flexible, point to a slight bending at the acid pH. This might be part of an adoption to the atomic structure of the E1 homotrimer, reported to be formed at acidic pH (Gibbons et al., 2004b). At a stage prior to target membrane interaction, there should be exposure of the fusion loop. This exposure is difficult to identify in the present structure, but would be located at the top of domain II (corresponding to node *c*), and be related to the movement of the node *c* observed in the spike head (**Fig. 18**).

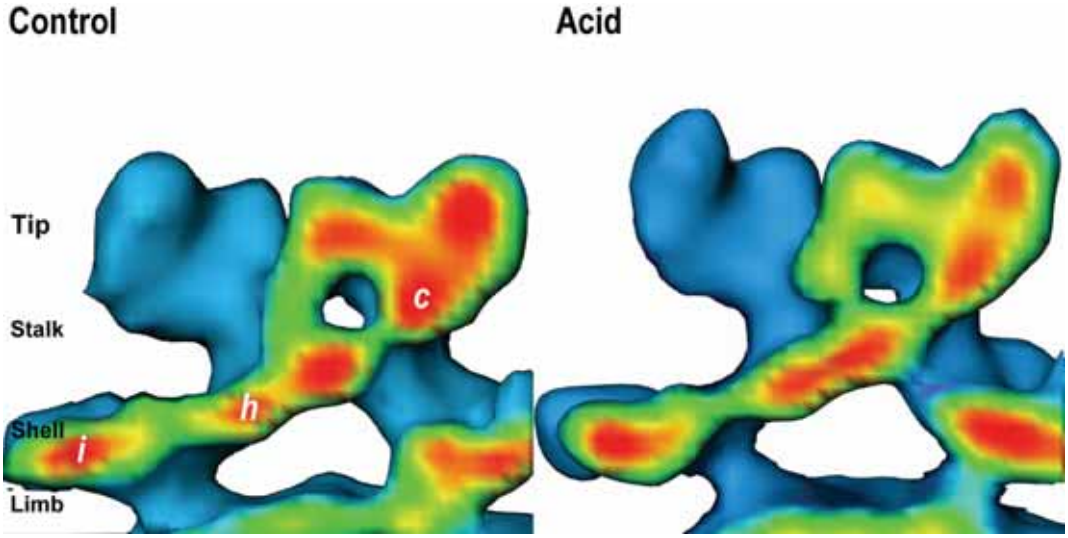

Figure 18. *Side views of the 3-fold spike cut along the direction of the E1 molecule.* Side views of the spikes as extracted from the acid and control virus reconstructions cut along the proposed location of the E1 molecule. The gradient color coding from blue to red represents σ=1 to 5 in the reconstructions. From the model fitting position of the domain III and domain I was assigned to the density node *i* and *h*, respectively. The density node *c* would correspond to the fusion loop according to the proposed model fitting of the E1 protein. Note the relocation of the density node *i* and the slimmer limb connections.

4.4 STRUCTURE OF FA INACTIVATED SFV (PAPER IV)

Cross-linking with FA is commonly used in the inactivation of whole virus vaccines and for fixation of biological specimen in structural studies. To explore how and to what extent FA influences or modifies the structures of a biological specimen we analyzed FA treated SFV using cryo-EM. Our goal was to establish conditions where the SFV infectivity was completely inactivated while causing minimal morphological damage. After an optimal condition for inactivation of gradient purified SFV was determined, cryo-EM micrographs FA treated particles were recorded and the structure determined. Differences in epitope accessibility in the treated compared to the control virus were evaluated using their pH-dependent MAb binding. We also tested whether

the FA treated SFV particles maintained their ability to induce cell-cell fusion from without – a test commonly used as a measure of virus membrane fusion capacity.

4.4.1 Result and discussion

During the screening for optimal FA concentration complete inactivation was achieved using a final concentration of 0.005 % FA, over 5 days at 20 °C, but not at 4 °C (**Fig. 19**, left). When the reaction was kept at 4 °C, a final FA concentration of 0.0125 % was required. This suggests that the FA inactivation reaction rate is temperature dependent (slower at the lower temperature) and that it could be compensated for by increased FA concentration. After selecting a FA concentration of 0.01 %, corresponding to roughly 350000 FA molecules per virion, the infectivity as a function of incubation time was followed. Complete SFV inactivation was achieved after 2 days incubation at 20 °C, while at 4 °C, the incubation time had to be prolonged for more than 4 days (**Fig. 19**, right). The infectivity was assessed in cell culture and detected using ELISA in which the presence of E2 proteins in the cell supernatant at 18 hours post-infection incubation was detected using an E2 antibody (MAbE2r). The quantity of newly produced E2 proteins was considered as a measure of infectivity. This measure of infectivity depends on the sensitivity of the ELISA and was therefore confirmed by the conventionally used and more established plaque assay (**Table 1**). The result from plaque assays of SFV, exposed to 0.01 % FA at 20 °C for 7 days, showed that the infectivity was reduced by roughly 9 orders of magnitude. We could also see, as reported in Table 1, that heating of the inactivated specimen to 56 °C did not reactivate the virus. Thus, the inactivation condition of 0.01 % FA at 20 °C for 7 days, produced complete inactivation as measured by two independent assays, and was used in subsequent experiments.

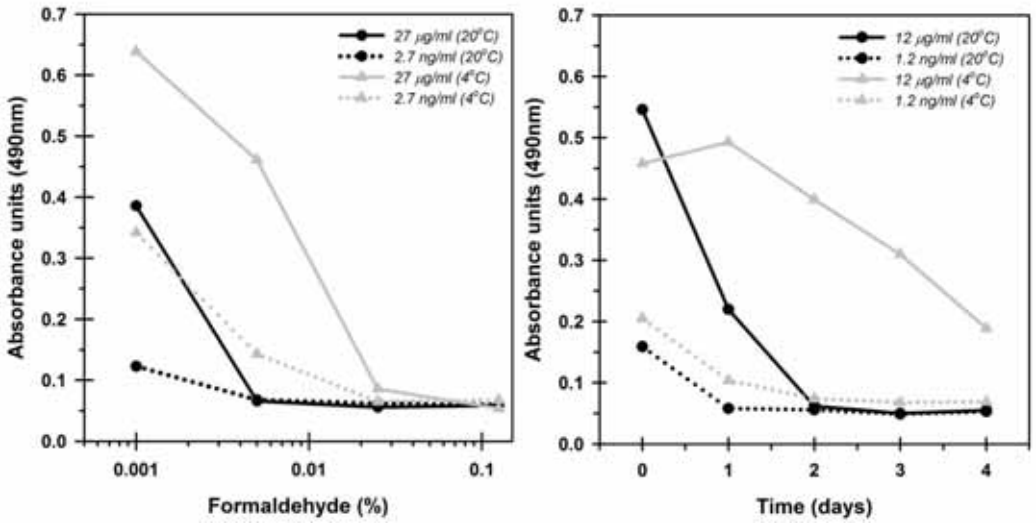

Figure 19. *Formaldehyde inactivation of SFV as a function of FA concentration and incubation time.* Aliquots of gradient purified SFV were incubated in the presence of 0.001-0.125 % FA at 4 °C or 20 °C for 5 days (left), or in the presence of 0.01 % FA for 1-4 days (right). Dilutions of the FA treated samples were tested for infectivity in BHK-21 cells. After 18 hours incubation the amount of expressed E2 protein detected in the cell supernatant, representing relative infectivity was measured by ELISA using an antibody against the E2 protein. The graphs show the relative infectivity (A_{490}) versus concentration of FA (left) or days of FA treatment (right). Different concentrations of the FA treated virus inoculum were used to emphasize the concentration dependence.

Sample	Titer (PFU/ml)
SFV	**$4.5x10^{11}$**
SFV_{FA}	**$4.5x10^{2}$**
SFV_{FA56}	**$< 4.5x10^{2}$**

Table 1. *Infectivity of FA treated SFV particles measured by plaque assay.* Plaque assay titers of FA treated SFV. Aliquots of purified SFV virus incubated in 0.01 % FA for 7 days at 20 °C (SFV_{FA}) and controls without FA (SFV) where diluted and analyzed in plaque assay on BHK-21 cells. A sample of the FA inactivated virus was heated to 56 °C for 10 min prior to the plaque assay (SFV_{FA56}). The table shows the virus titers as plaque forming unites per milliliter (PFU/ml) after the different treatments. Note that no reactivation occurred after heating to 56 °C.

FA is known as a cross-linking agent, therefore, we searched for cross-linked proteins as the possible cause for the established inactivation. This was analyzed by SDS-PAGE from which we observed that predominantly the C protein became chemically cross-linked (**Fig. 20**). The C protein was recovered as aggregates with a molecular mass above 250 kDa. No intermediate oligomeric forms or cross-linking to the E1 or E2 proteins were observed. This suggests that there had been both a specific and extensive C protein cross-linking reaction possibly involving the viral RNA. Cross-linking of the viral glycoproteins E1 and E2 occurred to a much lower extent as seen from the recovery of monomeric forms after sample heating to 56 °C or above (**Fig. 20**, below the gel).

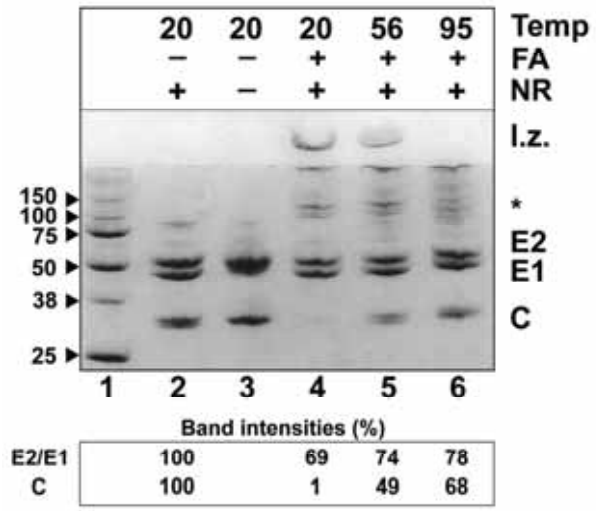

Figure 20. *Cross-linkage of SFV by FA treatment.* SDS-PAGE analysis of FA treated SFV. FA inactivated (lane 4 to 6) or untreated (lane 2 and 3) SFV where analyzed on a 20 % homogenous PhastGel™ and subsequently stained with Gelcode Blue. Prior to analysis the samples where heated to 20 °C (lane 2 to 4), 56 °C (lane 5) or 95 °C (lane 6) as shown above the gel. All samples were run under non-reducing (NR) conditions except lane 3. The positions of the material remaining in the loading zone (l.z.), monomeric (E2, E1 and C) and various oligomeric forms (*) of the viral proteins are indicated to the right. Note the reappearance of the monomeric form of the C protein when heated to 56 °C or above, and the concomitant disappearance of the aggregates in the sample loading zone. Band intensities corresponding to the monomeric forms of the viral proteins relative to bands in control, lane 2, are given below the gel.

Following the chemical characterization of the FA treatment we analyzed the effect of FA on selective MAb epitopes and their pH dependent accessibility. The viral epitopes were probed by our previously characterized MAbs (Hammar et al., 2003). These included epitopes in both the E1 and E2 glycoproteins. Among the epitopes within the E1 glycoprotein we found that the fusion loop, recognized by the MAbE1f, is partially exposed at close to neutral pH and becomes optimally accessible at an intermediate pH. The neutralizing antibody, MAbE1n, exhibited an opposite binding profile. This conformational epitope, recognized by the MAbE1n, was optimally exposed at neutral pH and became completely hidden below pH 6.0. Monoclonal antibodies against epitopes in the E2 protein showed generally an increased binding at acid pH. The MAbE2r, with specificity to an epitope close to the proposed receptor binding region bound in a two-step manner with a first binding maximum at pH 6.4 and a second one below pH 6.0. The control and inactivated virus samples displayed similar pH-dependent binding profiles, indicating a negligible effect of FA on the conformations of the probed epitopes in the external glycoproteins.

The effect of FA on the virions ability to induce cell-cell fusion, which we consider as a measure of biological function, was also analyzed. This assay would also, indirectly, reveal the degree of structural flexibility of the virus envelope and the proteins therein. Detailed analysis shows that approximately 80 % of the fusion capacity was preserved in the inactivated virus compared to the control virus (**Fig. 21**).

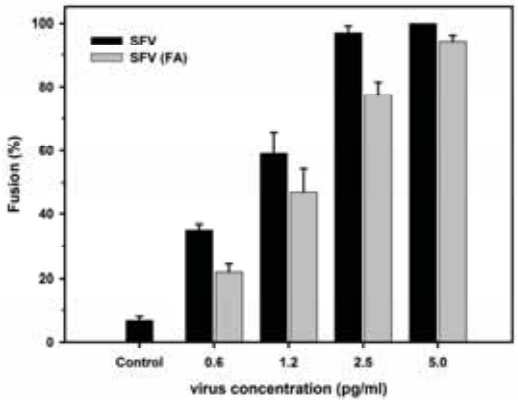

Figure 21. *SFV induced cell-cell fusion of BHK cells.* Extent of induced cell-cell fusion versus the inoculum concentration of control (black bars) and inactivated virus (grey bars). Cell-cell fusion was quantified by comparing the number of nuclei relative to the cells from images of fixed cells (fusion % = 1 - No. of cells / No. of nuclei x 100). The inoculum concentration was in the range of 0.6 to 5.0 pg/ml.

Image analysis of SFV particles, treated with 0.01% FA at 20 °C for 7 days, showed an overall well preserved virus morphology (**Fig. 22**). A 3D reconstruction averaged from 30 particles with a low-pass filter, set to suppress frequencies higher than 32 Å, showed an overall well preserved morphology. Morphological features in the native virus such as the characteristic spike-like protrusions, the shell layer with the openings at the 2- and 5-fold axes and the NC was similarly observed in the FA treated virus. Although heavily cross-linked, the hexameric and pentameric arrangement of the capsid proteins

was maintained in the NC. Considering that the virus was chemically modified to such an extent that its infectivity was completely abrogated, it is remarkable that both structural and functional features of the virion are so well retained.

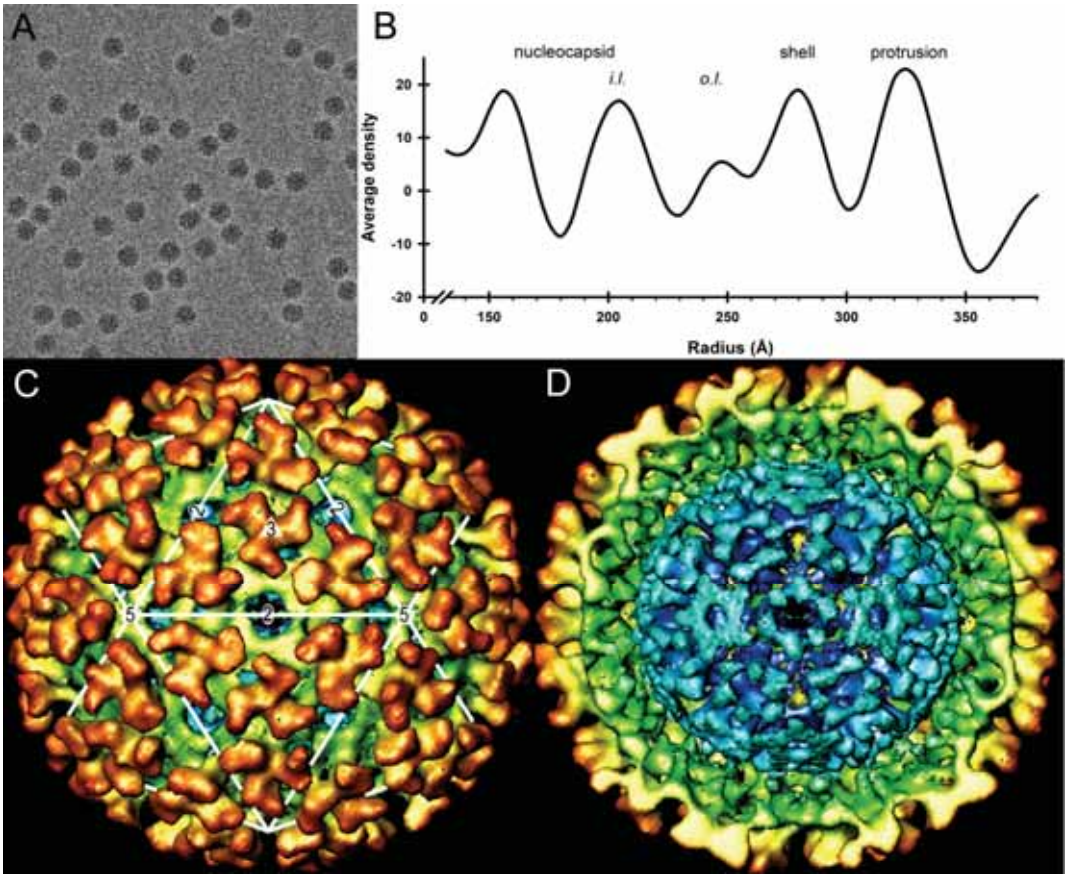

Figure 22. *Structure of a FA treated SFV virion.* Three-dimensional reconstruction of FA inactivated SFV. A Cryo-EM micrograph of inactivated SFV particles taken at -1 μm defocus and 28.000 nominal magnification (A). One-dimensional radial density distribution plot showing the characteristic density profile of the virus with peaks representing the spike protrusion, the shell domain, the outer (o.l.) and inner (i.l.) lipid layers of the membrane and the NC, as indicated (B). A two-fold surface view of the 3-D reconstruction showing the T=4 icosahedral arrangement of the protruding three-lobed spikes. Over-layered is an icosahedron showing symmetry related 5-, 3- and 2-fold axes (C). Cut-open view, from the spike to the sub-membrane domain, showing the internal arranged capsid proteins (D). The gradient color code represents the different layers of the virus.

4.5 EPITOPE MAPPING OF SFV SURFACE (UNPUBLISHED DATA I)

We have previously mapped a series of MAbs to linear epitopes in the SFV glycoprotein sequences. Several of these epitopes represent a specific biological function, as reported in *paper I*. To localize the epitopes in the SFV structure we prepared fab molecules to be used as structural probes in cryo-EM analysis. As reported in *paper I* most of the identified epitopes was shown pH sensitive and only accessible at pH below neutrality. Since the neutralizing MAbE1n bind the virus at neutral pH it was chosen for the first attempt to localize an epitope in the structure. To obtain a fab-virion complex, the gradient purified SFV was mixed with excess of the fab molecule

in a ratio corresponding to approximately four fab molecules per antigen, at neutral pH. The mixture were successively dialyzed to the optimal binding pH of 6.2 as identified in ELISA experiments, and incubated before removal of the excess of fab by gel filtration. Cryo-EM micrographs were recorded and analyzed, and a 30 Å resolution density map was computed.

4.5.1 Result and discussion

The conformational sensitive and neutralizing MAbE1n could not be mapped to a linear sequence. This IgG3 antibody was originally identified as an E1 antibody in WB. However, the specificity could be towards an E1-E2 dimeric structure. The exact composition of the site has not been conclusively identified. Its neutralization property was identified by the Salmi group, providing the hybridoma, and has been confirmed on freshly produced MAbs (Mattias Forsell, MTC, Karolinska Institutet). The MAbE1n shows strong binding to virus particles at neutral pH but the epitope becomes completely hidden for external binding at a pH below 6.2. This is confirmed both by Biacore experiments and ELISA. The antibody displays a similar pH-dependent binding profile to both the wild-type (wt) virus and the non-infectious SFVmSQL (data not shown). This suggests that the neutralizing epitope is not affected by the p62 cleavage and that both viruses share the same pH sensitivity at this site in the particle. The binding of the fab fragment was tested using Biacore, ELISA and WB to confirm that the cleavage of the antibody does not change the antigen binding property. In Biacore experiments it was shown to bind to immobilized virions in a ratio corresponding to one fab per spike (Hammar et al., 2003).

The 3D density map shows the virus structure with well-preserved overall virus morphology (**Fig. 23**, left). An additional external density can be seen as a halo surrounding the virus particle (**Fig. 23**, middle). From an enlargement of the 3-fold spike it is possible to see a tri-lobed density that converge from the center of the spike and that this is connected to the inner brim of the central spike cavity (**Fig. 23**, right). Assuming that the atomic resolution structure of the E1 protein has been correctly fit to our cryo-EM reconstructions, this density would correspond to the E2 protein. To definitely assign this density correctly, determination of mAbE1n antigen specificity is essential. An explanation for the diverged density is likely related to steric effects. Probably there is only space enough for one fab to bind per spike at this location. If the fab binds in a random and tilted orientation around the 3-fold axis it will give raise to such a diverged density since to virus will contain fab with a mixed binding orientations. Nevertheless, the density map shows the location of a conformational epitope that if occupied with an antibody is neutralizing (*i.e.* it prevents infection). Furthermore, accessibility of this epitope is not dependent on whether or not the p62 is cleaved, since the same relative occupancy is obtained with the SQL mutant.

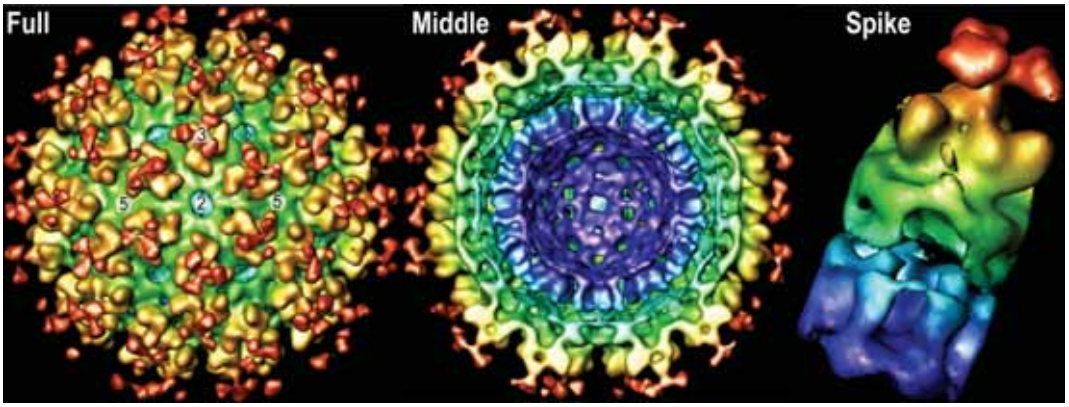

Figure 23. *Probing of a conformational sensitive neutralizing domain.* Three-dimensional structure of the wt SFV complexed with the fab fragment from the mAbE1n antibody. 2-fold views of the cryo-EM reconstruction of the surface (left), middle cross-section (middle) and a cut out of the 3-fold spike (right). The different symmetry related 2-, 3-, and 5-fold axes are shown on the surface view (left). The gradient color coding represents the radial position. The C protein (blue) with the N-terminus (dark blue) closest to the viral genome and the C-terminus (light blue) facing the inner lipid layer. Above the lipid bilayer is the limbs and shell domain (green) followed by the spike protrusion including the stalk (light green) and head (yellow). The tri-lobed shaped density above the spike (orange) is the additional density corresponding to the fab fragment. The shape of the density suggest a sub-stoichiometric binding occupancy, nevertheless, the binding is located in the central cavity of the spike.

4.6 SFV SUB-MEMBRANE DOMAIN (UNPUBLISHED DATA II)

In the SFV both glycoproteins penetrate the membrane with their C-terminals domains. The TM domains of the E1 and E2 have been described as two tilted α-helices (Mancini et al., 2000, Mukhopadhyay et al., 2006), Furthermore, the 31 aa long sub-membrane domain of E2, usually referred to as the (cytoplasmic)-tail (Garoff et al., 1980b) The E2-tail is interact with the C protein of the NC. We believe that this domain, which has been shown to be very important for the proper budding of the virion (Skoging et al., 1996, Skoging-Nyberg & Liljestrom, 2000, Zhao et al., 1994), also are important for the disintegration of the virus particle during membrane fusion. Therefore, we decided to perform a detailed analysis of the density corresponding to the sub-membrane domain in the 15 Å resolution density map of SFV at neutral pH. The density distribution at the 5-fold axis was continuously traced from the capsid protein, via the TM domains, to the outer lipid layer and the external limb structure (**Fig 24**).

4.6.1 Result and discussion

As indicated with the transparent area in the SFV structure surface rendering in **Figure 24A**, a tubular cut out of the densities surrounding the 5-fold axis is made to demonstrate the different layers of the virus and their details (**Fig. 24B**). The density of the limb domains are projecting to the underlying C protein monomers, but slightly shifted compared to the tilted TM domains (**Fig. 24B**, see TM region). At the outer lipid layer the limb densities seem to converge into a central 5-fold position, from where the TM domains originate (**Fig. 24B**, I). The shifted density direction between the limbs and TM is more obvious when looking at a cutout of the TM density (**Fig. 24B**, II). This shift in direction is due to that the tilted TM path originates from a more central 5-fold position in the outer lipid layer. A disk of the density around the 5-fold of

this domain, is cut as indicated by the transparent box, and tilted upwards (**Fig. 24B**, I). As can be seen from the figure (**Fig. 24B**, II) the TM domains indeed originate from a central density at the 5-fold axis in the outer lipid layer. Close to, or perhaps in the inner lipid layer the tilted TM domains again shift direction to become aligned with the C protein of the NC below the membrane (**Fig. 24B**, III). A density disk of this region was cutout and tilted downwards as indicated by the transparent box (**Fig. 24B**, III). This figure shows that after the contact to the C protein how it is possible to trace the density converging into a common 5-fold density in the sub-membrane space. This is likely the density corresponding to the E2 sub-membrane tail. The sub-membranuous density trace shows how it is possible to follow a structure emerging from the inner lipid layer, binds to the C protein, and subsequently joins in a central density (**Fig. 24B**, III). The corresponding density becomes weakened after acid pH treatment (see **Fig. 14** in *paper II*), which would reflect a dissociation of the contact between the E2 tail and the C protein. This has to be studied in detail in the acid structures. Here we show that also in the neutral structure there are details not previously identified or discussed. These observations should be examined further for their involvement in the fusion mechanism. At this stage, it is difficult to judge whether the observed expansion of the outer glycoprotein layer at acid pH is a consequence of a pH dependent dissociation of the close-to-membrane structures observed, or if it is the reorganization within the outer glycoprotein domains that affect the close to membrane and capsid interactions (compare signaling from without).

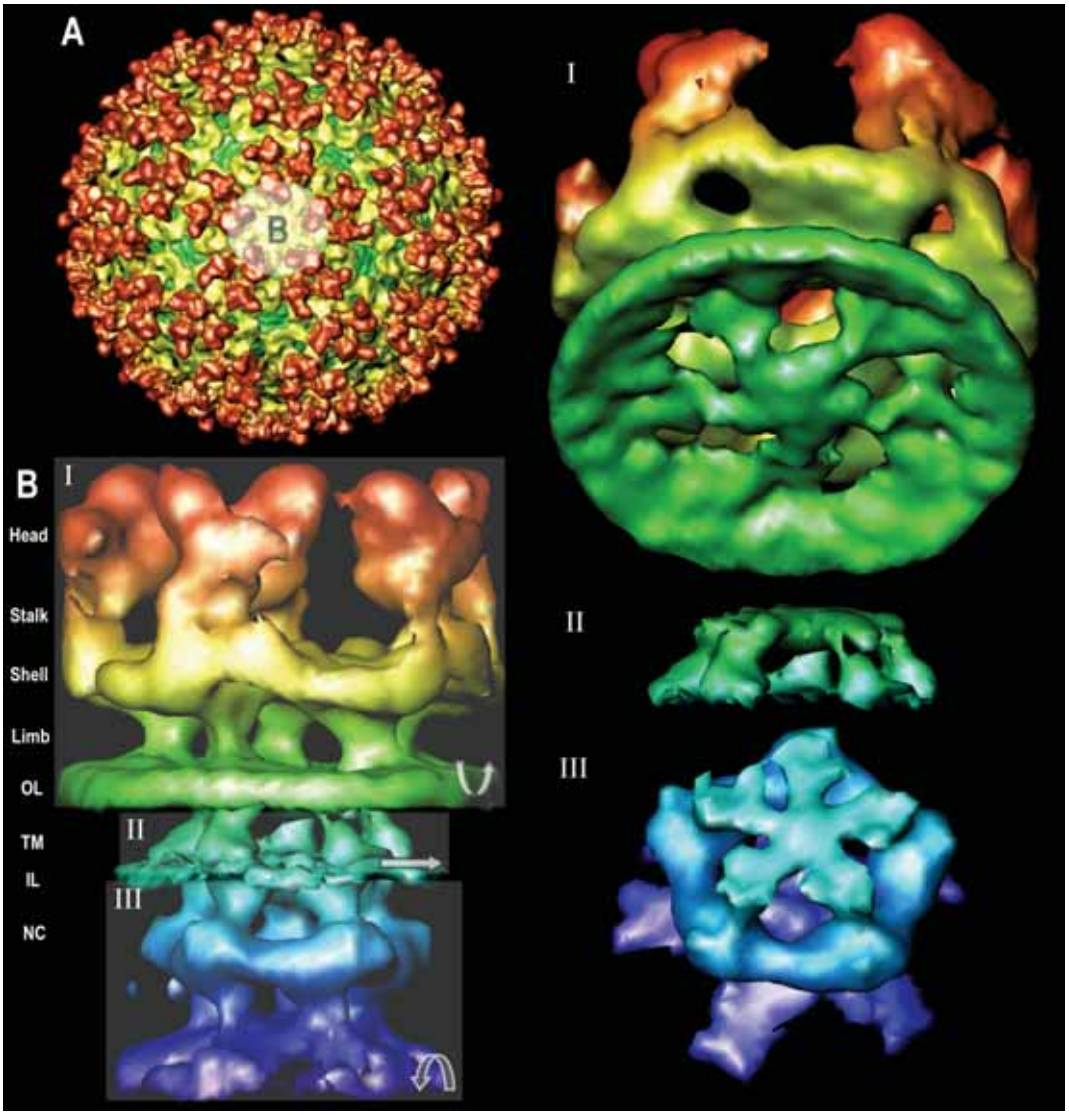

Figure 24. *Density trace from the shell to C protein of SFV.* (A) A surface rendering of a 15 Å SFV cryo-EM density map viewed along the 5-fold axis. A tubular cut is made, as indicated by the transparent surface B and shown in the figure below (B). (B) The 5-fold cut out shows the density distribution from the spike head (dark tan) to the top of the RNA layer (indigo) in which the N-terminal domain of the C protein is buried. The globular C-terminal domains of the C protein form the pentameric capsomer of the nucleocapsid (NC, blue). The different layers are denoted on the left hand side. Note the tilted TM domains and the connecting densities over the distance between the inner lipid layer and the capsid protein (NC). The transparent windows represent disks of the cut out; from the top of the spike protrusion to the outer lipid layer (I), the TM domain (II) and the inner lipid layer to the RNA layer (III). The tilted view of the disk I show how the limbs converge into a central 5-fold density not previously described. From this the tilted TM density domains originate (II) and end aligned to the position of the C protein monomers. The down tilted view of disk III shows the sub-membrane densities of the C protein and the E2-tail. Note how the density originating from the inner lipid layer above each C monomer, connects to the C protein and subsequently converge into a central 5-fold density.

4.7 GENERAL DISCUSSION AND FUTURE PERSPECTIVES

In this thesis I have focused on class II viral fusion mechanism, as it appears in SFV. The aim has been to reveal molecular alterations within the SFV particle that precede the actual fusion stage. This has been approached by structural and biochemical methods on an acid challenged virion. Among the tools that have been critical for obtaining the results are the antibody probes and their use in various binding

experiments, and the structural analyses of fusogenic intermediates by cryo-EM, 3D reconstruction, and molecular modeling. A chemical fixation technique was introduced in attempts to find means for safe specimen preparation and as an alternative approach to study the fusion process. Here I present the initial results with this method, but leave for the future to hook it on to the membrane-contact stage of fusion. In summarizing the results obtained, part of which have been presented in the papers and some only here, there are a few points that could be worth a continued discussion.

Alterations within the envelope of the E1 and E2 proteins

From the analysis of the control and acid pH density maps we observe molecular reorganizations that seem to be mainly located within the envelope glycoprotein layer. Based on the proposed model fitting of the E1 protein we have suggested that the differences in density distribution include an outward movement of the E1 concurrent with an alternative movement of a density assigned to the E2 protein, located in the spike stalk. This reciprocal movement of the two molecules would facilitate the exposure of the fusion loop at the outer side of the spike head, which is observed as an enhanced MAbE1f binding at the corresponding pH. However, the resolution of the density maps did not allow this level of detail to be seen. The same problem arose with the analysis of the virus-E1f fab complex analysis. Therefore, we cannot report an exact location of the site for the fusion loop, known to be exposed in the low pH structure.

Acid induced relocations of domains, denoted nodes, are observed to occur in the glycoprotein domains of the virus structure. The more prominent relocations are identified as dissolved contacts in the shell domain along with an elongation of the whole spike. In the spike the stalk region is undergoing a torsion whereby the trimeric contacts are opened in intervals. Within the bulky head of the spike, internal relocations of assigned nodes are observed. As indicated by our other studies these rearrangements are concomitant with the exposure of the fusion loop. The analyzed structures are reflecting a sequential transformation proceeding towards the fusogenic configuration of the virus. Still the spike heads are retained as morphological units in the acid structure. The slight relocations of the nodes reflect drastic functional changes, with variation in exposure of several hidden epitopes, including the fusion peptide (*Paper I*). Our observations show that the E2 protein controls the E1 domain II in more than one aspect; not only does it shield the fusion loop for external contacts at higher pH, it also stays in control at a late prefusion stage when the glycoprotein contacts in other domains are released.

Structural probes, epitopes and glycoconjugates

A set of monoclonal antibodies were characterized and mapped to sequential epitopes (*Paper I*). The epitopes represent regions of biological interest, such as the fusion loop, closeness to the receptor binding domain, a neutralizing domain and a domain close to the high-mannose glycoconjugate. These molecular probes are used in studies of the SFV to identify molecular alterations in the virus on controlled acidification. Moreover, attempts to structurally locate domains on the SFV surface using these antibodies as probes were performed. As discussed above (**Fig. 23**), the neutralizing site was located to the brim of the opening in the spike center (*unpublished data*). We observe that the bound MAbE1n is released below pH 6.2, suggesting that the neutralizing effect probably is affecting the virus cell interactions prior to internalization. The structural

targeting of remaining antibodies is a future task of high priority, in particular for the fusion loop directed antibody.

The extensive binding of GNA, which binds an average of three GNA per spike, suggests that all theoretical positions of its target, the high-mannose glycoconjugate in E2 (one site per E2 molecule), should be readily accessible at the virion surface. The fact that the glycoconjugate structure has remained non-trimmed and non-decorated throughout the ER-Golgi-PM budding pathway is remarkable, since regularly in proteins released from the cell the glycomoieties are extensively sialylated. The presence of a high-mannose conjugate in the mature virus is therefore either the result of an exhaustion of the cellular glycosylation machinery, or reflects that the conjugate is shielded during the secretory pathway, and made exposed at a late stage during maturation. The molecular mass of the GNA molecule is 52 kDa, i.e. similar to the mass of a fab fragment. Therefore, the steric availability for the binding of E1n and E1f fab fragments should be much more restricted than the lectin target. It is also to be noted that there are one N-glycosylation site, occupied with a complex type glycoconjugate, in each of the E1 and E2 glycoproteins. They may together with the high-mannose structure, form a shielding layer around the protein surface. Such shields are assumed to be strategic constructs allowing the virus to escape immune recognition.

Release of the NC contact with the envelope proteins
In the 15 Å resolution density map of SFV at neutral pH we could trace a density originating in the inner lipid layer, aligned to the C protein monomers, which after contact converged into a central density of the capsomers of the NC. The later could very well be the E2-tail. Densities corresponding to this submembrane structure became weakened after acid treatment. Dissociation of protein interactions in the region would involve the E2-tail and C protein contacts (Skoging-Nyberg & Liljestrom, 2001) and acidification could be a mechanism by which the envelope glycoproteins and NC are released. It is difficult to know whether the observed expansion of the outer glycoprotein layer is a consequence of the released contact in this region, or *vice versa* if the external reorganization within the E1/E2 glycoproteins affects the submembrane interaction (extracellular signaling). The loss of E2-tail to C submembrane contacts, along with released lateral control in the shell region, would facilitate a fluid relocation in the membrane of the two glycoproteins.

4.7.1 Prefusion stages

By studying prefusion stages in the native virion, as a full particle, our major o*bservations* are that 1) the fusion loop is exposed at an early stage during the fusogenic transformation, 2) the fusion protein E1 is not directly associated with the other E1 molecules in the same spike, 3) while allowing the exposure of the fusion loop, the E2 protein remains in control of the E1 top domain down to below pH 5.8. Thus the pH induced structural relocations primarily concern dissociation of the shell domain and the contacts between the E1 and E2 in the stalk domain of the spike. Our general interpretation of this is that the two glycoproteins collaborate beyond the stage of fusion peptide shielding to facilitate the fusion process.

1) Fusion loop is exposed at an early stage during the fusogenic transformation of SFV
The epitope for the MAbE1f (Y^{85}PFMWGGAYCF^{95}) is part of the fusion loop in the E1 protein, reported as the moderately hydrophobic sequence between Asp 75 and Asp 97 (D^{75}YQCKV YTGVYPFMWG GAYCFCD^{97} (Garoff et al., 1980b). Exposure of this epitope is seen at pH around 6.5, but it is optimally exposed at pH 5.9. This suggests that in the native particle the fusion loop is accessible for external interaction at a moderately acidic pH. At pH 6.0 an average of one fab molecule is bound per spike, as seen from the SPR saturation experiments. This is below the pH 6.2, reported as the SFV threshold for membrane fusion (Kielian & Helenius, 1984, White & Helenius, 1980a, White et al., 1980), and represents an environment where the virions appear non-aggregated and morphologically intact. Therefore, crucial functional changes in the accessibility of essential domains, like the fusion loop, might involve only subtle structural alterations. The low fab saturation of both the neutralizing site and the fusion peptide recognizing MAbs is likely an effect of steric hindrance. When the particles are exposed to pH below 5.8, aggregation of the virions occur. In preliminary experiments this aggregation is prevented if the MAbE1f is present during the acidification. On lowering the pH below 5.8 a higher proportion of exposed fusion loops, along with a less hydrophilic surface, may be the cause of the observed aggregation. However, a higher number of bound fabs have, so far, not been confirmed.

A note on the antibody and the pH. The binding of an antibody to its epitope is depending on biospecific affinity, and on the accessibility of the epitope. The biospecific affinity would be dependent on the environmental pH, which could also be the case for the accessibility in a dynamic structure. Therefore, the interactions that we here recall would reflect both parameters. All the MAbs discussed here bind the virus proteins at neutral or close to neutral pH in WB. The MAbE1n, gives a week binding in WB and does not bind to the Pepscan peptides, in contrast it binds well to the virus at close to neutral pH in ELISA and Biacore experiments. The E1n does not bind the virus at acid pH, but virus binding can be regained if the virus was exposed to acid conditions for a short time, but not extensively, prior to MAb binding at neutral pH. This point to that it is fluctuations in the virus that determines if the antibody binds or not. Furthermore, the epitope is completely lost if the virus particles are treated with low concentrations of non-ionic detergents like NP-40, again showing the conformational sensitivity of this MAb. The other MAbs that interact with the acidified virus, all bind well to denatured virus proteins at pH 7.4. Therefore, the major factor for binding to respective antigen, in the range studied, is the epitope accessibility on the surface of the virus. This does not exclude that other antibodies, not used here, might have a different window of activity.

2) Fusion protein E1 is not associated with other E1 molecules in the same spike
One may ask what that means in relation to the present views on the class II fusion mechanism. If a homotrimer of the fusion protein is necessary for the fusion to occur, how, and at what stage is it formed? In the fusion class I case, as studied in the Influenza virus and HIV, the fusion protein is initially present as an internal homotrimer within the spike, prior to fusion activation. This seems not to be the case with the E1 fusion protein of the SFV, representing class II fusion mechanism. Based on the current structure of the SFV at neutral and acidic pH, and the modeled fitting of the E1 atomic structure, the only external contacts between the fusion proteins are in the shell layer. There the contacts are between different spikes. In the spike itself, the

E2 protein forms the connections, linking the E1-E2 heterotrimer. Therefore, a major obstacle for the reorganization into an E1 homotrimer form is the E2 protein. In the influenza case the interference by HA1 is different – the release of the N-terminal fusion peptide in the HA1, would result in a drastic relocation to produce the earlier hidden fusion peptide on top of a protruding triple helix bundle. In this action the initial trimeric organization is retained. However, in the E1 case, a quite different reshuffling of the two glycoproteins seems to be needed.

3) E2 protein remains in control of the E1 in the spike head to secure the fusion loop
It has been reported that before reaching pH 5.9, in the presence or absence of liposome membranes, the viral spike undergo dissociation of E1-E2 dimers before trimerization of the E1 protein (Wahlberg et al., 1989, Wahlberg et al., 1992, Wahlberg & Garoff, 1992). Therefore, we expected to detect significant protein refoldings, corresponding to the reported conversion into the fusion active conformation. In our hands the acid pH-induced conversion of the particles involved transformations into particles of different sizes. The different forms could be differentiated during the particle image selection from the cryo-EM micrographs by real space size classification. It was found that the virus adapted a larger size at the more acidic pH. From the 3D reconstructions obtained at different pH the structure could be followed at stages down to pH 5.8. As discussed in *paper II* we conclude that at the pH of 5.8, when the virus is highly prone for interaction with a target membrane, the contact between the two proteins are mainly confined to the tip of the spikes and the shell-limb region. Thus, while the E1-E1 lateral contacts in the shell are dissociating between the spikes, and the stalk interactions are opening up, the E1-E2 contacts in the head of the spikes are not released. Therefore, the formation of an E1 homotrimer is far from complete, or even easily possible. The E1 and E2 glycoproteins appear to keep together in the spike structure in spite of the fact that the fusion peptide is exposed. The two proteins might well dissociate in the presence of a target membrane, but that is something that we have not been able to control.

4.7.2 Considerations on the class II mechanism

What is the driving force for the relocations seen?
Is the answer the shell expansion? Acidified virions expand, while the membrane remains essentially at the same radius. This includes widening of the shell. The structural origin of this expansion is unclear; it may result from elongation of the limbs, from lateral expansion within the shell itself or be a result of a demand for wider angles of the structures above.
The expansion occurs as a result of a lowered pH. Generally, in peptides at neutral pH the side chains of arginine and lysine, along with the N-terminal amino group, are positively charged. Towards lower pH the histidine side chain become protonated, with a pKa of 6.0, and provides a positive charge. Towards a lower pH the carboxyl groups of aspartic and glutamic acids are also protonated (pKa 3.7-4.2, highly dependent on the local environment) and lose their negative charge. Therefore, in the range below neutral the first pH-related event would be the appearance of positively charged histidyl resides.

A cluster of His is found at the interphase of DI and DIII in the E1* structure. The contributing residuals are His 3 (conserved) and His 18 in the DI and His 331 (conserved) and His 333 (partly conserved) in the DIII. The distances between them are between 3.7 and 5.2 Å (Roussel et al., 2006). In the virus this would be located at the inside of the shell, in the cleft between nodes *h* and *i*. It is tempting to assume that the distortion seen in this domain in the acid structure (*Paper III*, **Fig. 18**) is the result of repulsion by the acquired positive charges. As a theoretical construct, an expansion of the shell would result in both the extension and narrowing of the limbs and the lift of the whole external domain. The impact of this would be that DIII is released from DI with no other contacts between them than the long connecting sequence. (At the same time its lateral contact with other similar domains of adjacent spikes are lost.)

Other His sites are located close to the limb extension in the DIII, the E1-E2 interface in the stalk region, in the dimeric contacts between the spikes in the shell region, and close to the location for the assumed cholesterol determinant (Pro 226) in the node *c*. In all these locations there are small but distinct relocations between nodes that occur on acidification. The number of His in the E1 sequence is 13 residues, which is only 2.9 % of its total number of amino acids (438), while there are 23 His in the E2 protein, which is 5.5 % of the total (422). Therefore, the E2 protein would be much more sensitive to the protonization of histidine. Unfortunately, we do not yet have the folding information of E2 needed to draw conclusions about its electrostatic configuration.

Are there indications of an E1 homotrimer formation?
From the atomic structure of acid triggered E1 homotrimer a jack-knife-like relocation of domain III and a bending of domain II is proposed (Gibbons et al., 2004b). These drastic molecular reorganizations cannot be seen in our 3D reconstructions and might represent a configuration only attainable in the presence of a target membrane, or possibly as a post fusion structure. What can be found in the virus structures is that the first criterion is partly met, that is the released DIII freeing itself from the DI, except for the linker sequence connection. Such an independent movement of the DIII would be necessary to establish a contact to DII of neighboring E1 molecules before or after E1 trimerization. This type of contact is probably essential for the fusion to proceed after the fusion loop has been inserted in the target membrane, since it is found that separately added DIII molecules acts as inhibitors for infection, and membrane mergence (Liao & Kielian, 2005). A parallel is found in the neutralization of JEV by antibodies directed against this site in the DII of JEV molecule. In this case the neutralization was effective at a late stage of infection (Butrapet et al., 1998), after cell binding, as discussed in (Abe et al., 2006). An additional observation is an initiation of a bending in the hinge region of the E1 molecule, directed towards the kink found in the homotrimers of external E1 (E1*HT). In *paper III*, model fitting show that there should be a bend at the hinge region of about 6° to fit into the acid structure while 15° is observed in the E1*HT. This might not be a high fidelity observation since the model fitting was done in an intermediate resolution density map, but could still give an indication of a reorganization of the E1 protein.

It is still not fully clear whether E1 homotrimers are formed prior to membrane interaction, are formed during the actual fusion process, or if the trimers are a post-fusion phenomenon found only in the fused membranes (Bron et al., 1993, Wahlberg et

al., 1992). It has been shown that exposure of SFV particles to acid pH, in the absence of cholesterol containing target liposomes, lead to the formation of E1 homotrimers in similar extent as in the presence of liposomes (Wahlberg et al., 1992). This suggests that the acid pH triggered conformational reorganizations leading to E1 trimerization also occur in the SFV particles in the absence of a target membrane. In the same study they show that a noninfectious mutant (mL), in which the p62 precursor protein is prevented from being proteolytically cleaved into the E2 and E3 proteins, were unable to expose the acid sensitive anti-E1" epitope and forming E1 homotrimers after low pH treatment. After proteolytic activation *in vitro* by trypsin it displayed similar epitope accessibility and E1 trimerization as the wild-type virus. A similar cleavage deficient SFV mutant (SQL) with two additional upstream mutations regained full infectivity already after limited proteolytic cleavage (Berglund et al., 1993). This suggests that a small number of mature spikes are enough to restore the full infectivity. The likelihood of E1 trimerization to occur specifically in the spikes around the 5- or 2-fold axis after the unspecific cleavage of the p62 would be low. Therefore, it is still uncertain to what degree E1 homotrimer reorganization is involved in the membrane fusion process. From the crystallization study of the E1 homotrimer it was suggested that a pentameric form of E1 homotrimers would be involved to cooperatively force the target membrane in close proximity with the viral membrane (Gibbons et al., 2003). Mechanistically this asymmetric bending of the target membrane is difficult to foresee. Therefore, if the E1 homotrimers are formed prior to membrane fusion it remains to be found how they perform their role in the fusion process. Several attempts to access the pH-induced structural dynamics in the virus in the absence of target membranes have been made but no conclusive results was found (Fuller et al., 1995, Haag et al., 2002, Paredes et al., 2004).

Approaching the membrane anchored state

The inactivation of SFV with formaldehyde in optimized condition reduces the infectivity by 9 $\log_{10}$. The loss of infectivity was achieved at conditions were the overall virus morphology was well preserved as seen by 3D reconstruction from cryo-EM micrographs. The FA reaction preferentially cross-linked the C protein into large aggregates while the in the native virion tightly connected viral envelope proteins, E1 and E2, were cross-linked to a much less degree. The partial cross-linkage of the surface proteins did not prevent their fusion related structural reorganizations, triggered by low pH. The substantial cross-linkage of the sub-membranous capsid proteins, and the maintained integrity of the virus surface, indicate that the loss of infectivity was not due to a biologically non-functional virus envelope. Speculations that the inactivation affect a late stage of the infection process is supported by the low impact of FA treatment on pre-fusion rearrangement of epitopes, including the fusion loop exposure, and the capacity to trigger cell-cell fusion. In summery, we speculate that the actual inactivation by formalin on SFV infectivity is an effect of intra-capsid cross-linkage, possibly including the viral genome. This would result in a rigid NC from which the genome release into the cytoplasm of the host-cell during infection is impeded, but leaving the envelope rather intact.

If a short pulse of FA is enough for cross linking the NC, or at least the RNA, without altering the dynamics of the external protein layer, then this could be used to prepare virions that bind to liposomes but that do not release the genome. Thereby it would be

possible to trap early stages of the fusion reaction. This would allow us to find out if E1 trimers are necessary or not for membrane anchoring, and if pores might alternatively form, instead of complete membrane merging. This has relevance, since it is known that the E1 protein, expressed alone can form pores in bacterial membranes (Nyfeler et al., 2001). However, in this case it is not well established how the E1 is inserted in the bacterial membrane, since it may not have a proper signal sequence.

The insight in SFV fusion mechanism established in this study put forward details of the class II fusion mechanism not earlier anticipated. What we have shown are structural relocations not earlier explored in the full virion. I believe that, even though our observations presented in this thesis take us a little further into an understanding of this type of fusion mechanism, there are and will be many more questions to answer. The tools to be used in future studies may well include structural probing using fab molecules and various virus mutants, like the fusion deficient mSQL. Furthermore, to explore membrane anchored fusion intermediates, nucleic acid cross-linking, like what is achieved with formaldehyde, may facilitate a continued structural study.

5 ACKNOWLEDGEMENTS

I have many people to thank for help and support during the work of my thesis. I am grateful to you all, in particular I want to thank:

Professor Holland R. Cheng, for having the belief in me to mature independently and develop a critical mind.

Associate Professor Lena Hammar, you have been the most important person for me during these years, helping me both practically and mentally. For all you have done for me, I am deeply grateful. I wish you all the best writing your "book", which I will be the first one to buy.

Present and former colleagues in the HCH-group;

Josefina Nilsson, to have had you as a co-worker has been a privilege and made these years worth spending. Despite all the hard work and "scientific discussions" I think we always kept a good spirit. I am sure that the friendship we have developed will continue for long time.

Sunny Wu, I hope the time we spent together in the lab will take you over the hill (although that hill sometimes might look like Mount Everest). I really admire the strength and determination you possess and wish you all the best in your future studies.

Joe Wang, I really wished you could have stayed in the lab a little longer. With your competence I am sure you will finish your studies soon. Be careful with the wine though, those whiplash injuries are not good for your neck.

Leif Bergman, you seem to just absorb knowledge about everything and in your case it actually sticks. Thank you for always have taken the time to answer all the annoying and stupid questions from a "hacker wannabe".

Bomu Wu, for teaching me all about cryo-EM image analysis. I wish you and your family all the best.

Dr. David Morgan, for proof-reading of the thesis. Even though we met for such a short time I found a true friend in you. Probably, there will soon be other students in need.

Dr. Li Xing, for sharing the lab together and all nice micrographs you have recorded. Sorry there was no time for any goodbyes. I wish you all the best in your future career.

Finally, a to all former group members not mentioned above that I have had the opportunity to work with; **Sin-Tau, Anders, Nicklas, Ruchi, Naoyuki, Igor, Wit, Fredrik, Helena E, Helena S, Kicki, Anna, Willhem** and **Sevak**.

Colleagues in the HGA-group;

Professor Henrik Garoff, for the scientific discussions and continuous support. I really appreciate your genuine interest and help in the field of structural virology.

Mathilda Sjöberg, without all your help with the Semliki Forest virus this project would not have been possible.

Birgitta Lindqvist, the living Finish (from Karelen) biotech encyclopedia with the fastest eppendorff thumbs I have ever seen. You are the ONE person that impressed me the most. Your knowledge, humor, positive energy, helpfulness well you name it, have really helped me through these years. Watch out for tall silent men with cold necks that move slowly.

Ylva Rabo, for maintaining such a nice cell and virus facility and for always providing me with excellent cell cultures.

Rickard Nordström, the sewing machine will always be there for you, and if you need another "clone replicator" just call me. **Robin Löving**, don't forget to exchange the S to an R on your superman outfit, you "R-peptideman". It has really been an injection having you guys around. **Maria Hammarstedt**, I will pass on the "relay stick" to remind you on what soon will come, a paradise with mooses waits around the corner. Last but not least **Mikael, Maria E, Helena, Malin, Kejun** and **Shujin** for there support during all these years.

Cesar Santiago, the cool cool "kalimotxo guy". Watch out, I'll be knocking on your door when you least expect it. It was really fun having a little Spanish flavour around.

Inger[3] (Moge, Ericsson and Palm), Novums true sunbeams, what will I do without your morning hi's that always got me in good mood and made me feel welcome. Be careful with those green bags though and please try to lift those heavy feet.

Mohammed Homman, having met you and your family is a privilege. You are one of the most complete, energetic, inventive and fun person I have ever met.

People outside the academic world:

All my closest friends **Keivan, Niclas, Jonas & Linda, Fredrik & Renèe, Henrik & Charlotta, Martin & Susanne, Torben & Catti** you have filled these years with other and more important things than viruses.

My sisters, **Anna** and **Astrid** with families, I have the best sisters in the world with the nicest families. I hope we can meet somewhat more frequent now.

My parents, **Märtha** and **Börje**, for your endless support and love. I really want to express my deepest appreciation for your continuous encouragement.

Cilla, the love of my life. You have gone through years of ups and downs but always been there for me. At last we can proceed into a new phase in our lives with whatever that awaits us.

6 REFERENCES

Abe, M., Shiosaki, K., Hammar, L., Sonoda, K., Xing, L. & Kuzuhara, S. (2006). Immunological equivalence between mouse brain-derived and Vero cell-derived Japanese encephalitis vaccine. *Virus Research* **Submitted**.

Acheson, N. H. & Tamm, I. (1967). Replication of Semliki Forest virus: an electron microscopic study. *Virology* **32**, 128-43.

Ahn, A., Gibbons, D. L. & Kielian, M. (2002). The fusion peptide of Semliki Forest virus associates with sterol-rich membrane domains. *J Virol* **76**, 3267-75.

Aliperti, G. & Schlesinger, M. J. (1978). Evidence for an autoprotease activity of sindbis virus capsid protein. *Virology* **90**, 366-9.

Baker, T. S. & Cheng, R. H. (1996). A model-based approach for determining orientations of biological macromolecules imaged by cryoelectron microscopy. *J Struct Biol* **116**, 120-30.

Barth, B. U., Wahlberg, J. M. & Garoff, H. (1995). The oligomerization reaction of the Semliki Forest virus membrane protein subunits. *J Cell Biol* **128**, 283-91.

Berglund, P., Sjoberg, M., Garoff, H., Atkins, G. J., Sheahan, B. J. & Liljestrom, P. (1993). Semliki Forest virus expression system: production of conditionally infectious recombinant particles. *Biotechnology (N Y)* **11**, 916-20.

Bressanelli, S., Stiasny, K., Allison, S. L., Stura, E. A., Duquerroy, S., Lescar, J., Heinz, F. X. & Rey, F. A. (2004). Structure of a flavivirus envelope glycoprotein in its low-pH-induced membrane fusion conformation. *Embo J* **23**, 728-38.

Bron, R., Wahlberg, J. M., Garoff, H. & Wilschut, J. (1993). Membrane fusion of Semliki Forest virus in a model system: correlation between fusion kinetics and structural changes in the envelope glycoprotein. *Embo J* **12**, 693-701.

Bullough, P. A., Hughson, F. M., Skehel, J. J. & Wiley, D. C. (1994). Structure of influenza haemagglutinin at the pH of membrane fusion. *Nature* **371**, 37-43.

Butrapet, S., Kimura-Kuroda, J., Zhou, D. S. & Yasui, K. (1998). Neutralizing mechanism of a monoclonal antibody against Japanese encephalitis virus glycoprotein E. *Am J Trop Med Hyg* **58**, 389-98.

Byrnes, A. P. & Griffin, D. E. (1998). Binding of Sindbis virus to cell surface heparan sulfate. *J Virol* **72**, 7349-56.

Chatterjee, P. K., Vashishtha, M. & Kielian, M. (2000). Biochemical consequences of a mutation that controls the cholesterol dependence of Semliki Forest virus fusion. *J Virol* **74**, 1623-31.

Cheng, R. H., Kuhn, R. J., Olson, N. H., Rossmann, M. G., Choi, H. K., Smith, T. J. & Baker, T. S. (1995). Nucleocapsid and glycoprotein organization in an enveloped virus. *Cell* **80**, 621-30.

Choi, H. K., Lu, G., Lee, S., Wengler, G. & Rossmann, M. G. (1997). Structure of Semliki Forest virus core protein. *Proteins* **27**, 345-59.

Choi, H. K., Tong, L., Minor, W., Dumas, P., Boege, U., Rossmann, M. G. & Wengler, G. (1991). Structure of Sindbis virus core protein reveals a chymotrypsin-like serine proteinase and the organization of the virion. *Nature* **354**, 37-43.

Dimitrov, D. S. (2004). Virus entry: molecular mechanisms and biomedical applications. *Nat Rev Microbiol* **2**, 109-22.

Duffus, W. A., Levy-Mintz, P., Klimjack, M. R. & Kielian, M. (1995). Mutations in the putative fusion peptide of Semliki Forest virus affect spike protein oligomerization and virus assembly. *J Virol* **69**, 2471-9.

Fan, D. P. & Sefton, B. M. (1978). The entry into host cells of Sindbis virus, vesicular stomatitis virus and Sendai virus. *Cell* **15**, 985-92.

Ferlenghi, I., Gowen, B., de Haas, F., Mancini, E. J., Garoff, H., Sjoberg, M. & Fuller, S. D. (1998). The first step: activation of the Semliki Forest virus spike protein precursor causes a localized conformational change in the trimeric spike. *J Mol Biol* **283**, 71-81.

Forsell, K., Suomalainen, M. & Garoff, H. (1995). Structure-function relation of the NH2-terminal domain of the Semliki Forest virus capsid protein. *J Virol* **69**, 1556-63.

Forsell, K., Xing, L., Kozlovska, T., Cheng, R. H. & Garoff, H. (2000). Membrane proteins organize a symmetrical virus. *Embo J* **19**, 5081-91.
Fuller, S. D., Berriman, J. A., Butcher, S. J. & Gowen, B. E. (1995). Low pH induces swiveling of the glycoprotein heterodimers in the Semliki Forest virus spike complex. *Cell* **81**, 715-25.
Gaedigk-Nitschko, K. & Schlesinger, M. J. (1990). The Sindbis virus 6K protein can be detected in virions and is acylated with fatty acids. *Virology* **175**, 274-81.
Garoff, H., Frischauf, A. M., Simons, K., Lehrach, H. & Delius, H. (1980a). The capsid protein of Semliki Forest virus has clusters of basic amino acids and prolines in its amino-terminal region. *Proc Natl Acad Sci U S A* **77**, 6376-80.
Garoff, H., Frischauf, A. M., Simons, K., Lehrach, H. & Delius, H. (1980b). Nucleotide sequence of cdna coding for Semliki Forest virus membrane glycoproteins. *Nature* **288**, 236-41.
Garoff, H., Hewson, R. & Opstelten, D. J. (1998). Virus maturation by budding. *Microbiol Mol Biol Rev* **62**, 1171-90.
Garoff, H. & Simons, K. (1974). Location of the spike glycoproteins in the Semliki Forest virus membrane. *Proc Natl Acad Sci U S A* **71**, 3988-92.
Garoff, H., Sjoberg, M. & Cheng, R. H. (2004). Budding of alphaviruses. *Virus Res* **106**, 103-16.
Geigenmuller-Gnirke, U., Nitschko, H. & Schlesinger, S. (1993). Deletion analysis of the capsid protein of Sindbis virus: identification of the RNA binding region. *J Virol* **67**, 1620-6.
Gibbons, D. L., Ahn, A., Liao, M., Hammar, L., Cheng, R. H. & Kielian, M. (2004a). Multistep regulation of membrane insertion of the fusion peptide of Semliki Forest virus. *J Virol* **78**, 3312-8.
Gibbons, D. L., Erk, I., Reilly, B., Navaza, J., Kielian, M., Rey, F. A. & Lepault, J. (2003). Visualization of the target-membrane-inserted fusion protein of Semliki Forest virus by combined electron microscopy and crystallography. *Cell* **114**, 573-83.
Gibbons, D. L., Vaney, M. C., Roussel, A., Vigouroux, A., Reilly, B., Lepault, J., Kielian, M. & Rey, F. A. (2004b). Conformational change and protein-protein interactions of the fusion protein of Semliki Forest virus. *Nature* **427**, 320-5.
Greber, U. F., Singh, I. & Helenius, A. (1994). Mechanisms of virus uncoating. *Trends Microbiol* **2**, 52-6.
Griffiths, G., Fuller, S. D., Back, R., Hollinshead, M., Pfeiffer, S. & Simons, K. (1989). The dynamic nature of the Golgi complex. *J Cell Biol* **108**, 277-97.
Griffiths, G. & Gruenberg, J. (1991). The arguments for pre-existing early and late endosomes. *Trends Cell Biol* **1**, 5-9.
Grimley, P. M., Berezesky, I. K. & Friedman, R. M. (1968). Cytoplasmic structures associated with an arbovirus infection: loci of viral ribonucleic acid synthesis. *J Virol* **2**, 1326-38.
Haag, L., Garoff, H., Xing, L., Hammar, L., Kan, S. T. & Cheng, R. H. (2002). Acid-induced movements in the glycoprotein shell of an alphavirus turn the spikes into membrane fusion mode. *Embo J* **21**, 4402-10.
Hammar, L., Haag, L., Wu, B. & Cheng, R. H. (2004). Prefusion dynamics in an enveloped virus - Alphavirus model. *Conformational proteomics of macromolecular architecture; Approaching the structure of large molecular assemblies and their mechanisms of action. (World Scientific Publishing CO. Pte. Ltd., Singapore, 2004)*, 78-108.
Hammar, L., Markarian, S., Haag, L., Lankinen, H., Salmi, A. & Cheng, R. H. (2003). Prefusion rearrangements resulting in fusion Peptide exposure in Semliki forest virus. *J Biol Chem* **278**, 7189-98.
Helenius, A. & Kartenbeck, J. (1980). The effects of octylglucoside on the Semliki forest virus membrane. Evidence for a spike-protein--nucleocapsid interaction. *Eur J Biochem* **106**, 613-18.
Helenius, A. & Marsh, M. (1982). Endocytosis of enveloped animal viruses. *Ciba Found Symp*, 59-76.
Helenius, A., Morein, B., Fries, E., Simons, K., Robinson, P., Schirrmacher, V., Terhorst, C. & Strominger, J. L. (1978). Human (HLA-A and HLA-B) and

murine (H-2K and H-2D) histocompatibility antigens are cell surface receptors for Semliki Forest virus. *Proc Natl Acad Sci U S A* **75**, 3846-50.
Ivanova, L. & Schlesinger, M. J. (1993). Site-directed mutations in the Sindbis virus E2 glycoprotein identify palmitoylation sites and affect virus budding. *J Virol* **67**, 2546-51.
Jain, S. K., DeCandido, S. & Kielian, M. (1991). Processing of the p62 envelope precursor protein of Semliki Forest virus. *J Biol Chem* **266**, 5756-61.
Karnovsky, M. J. (1965). A formaldehyde-glutaraldehyde fixative of high osmolarity for use in electron microscopy. *J. Cell Biol.* **27**, 137-138.
Kenney, J. M., Sjoberg, M., Garoff, H. & Fuller, S. D. (1994). Visualization of fusion activation in the Semliki Forest virus spike. *Structure* **2**, 823-32.
Kielian, M. (1995). Membrane fusion and the alphavirus life cycle. *Adv Virus Res* **45**, 113-51.
Kielian, M. & Rey, F. A. (2006). Virus membrane-fusion proteins: more than one way to make a hairpin. *Nat Rev Microbiol* **4**, 67-76.
Kielian, M. C. & Helenius, A. (1984). Role of cholesterol in fusion of Semliki Forest virus with membranes. *J Virol* **52**, 281-3.
Kielian, M. C., Keranen, S., Kaariainen, L. & Helenius, A. (1984). Membrane fusion mutants of Semliki Forest virus. *J Cell Biol* **98**, 139-45.
Kiernan, J. A. (2000). Formaldehyde, formalin, paraformaldehyde and glutaraldehyde: What they are and what theu do. *Microscopy today*, 8-12.
Kujala, P., Ikaheimonen, A., Ehsani, N., Vihinen, H., Auvinen, P. & Kaariainen, L. (2001). Biogenesis of the Semliki Forest virus RNA replication complex. *J Virol* **75**, 3873-84.
Laemmli, U. K. (1970). Cleavage of structural proteins during the assembly of the head of bacteriophage T4. *Nature* **227**, 680-5.
Lescar, J., Roussel, A., Wien, M. W., Navaza, J., Fuller, S. D., Wengler, G. & Rey, F. A. (2001). The Fusion glycoprotein shell of Semliki Forest virus: an icosahedral assembly primed for fusogenic activation at endosomal pH. *Cell* **105**, 137-48.
Levy-Mintz, P. & Kielian, M. (1991). Mutagenesis of the putative fusion domain of the Semliki Forest virus spike protein. *J Virol* **65**, 4292-300.
Liao, M. & Kielian, M. (2005). Domain III from class II fusion proteins functions as a dominant-negative inhibitor of virus membrane fusion. *J Cell Biol* **171**, 111-20.
Liljestrom, P. & Garoff, H. (1991). A new generation of animal cell expression vectors based on the Semliki Forest virus replicon. *Biotechnology (N Y)* **9**, 1356-61.
Liljestrom, P., Lusa, S., Huylebroeck, D. & Garoff, H. (1991). In vitro mutagenesis of a full-length cDNA clone of Semliki Forest virus: the small 6,000-molecular-weight membrane protein modulates virus release. *J Virol* **65**, 4107-13.
Lobigs, M. & Garoff, H. (1990). Fusion function of the Semliki Forest virus spike is activated by proteolytic cleavage of the envelope glycoprotein precursor p62. *J Virol* **64**, 1233-40.
Loewy, A., Smyth, J., von Bonsdorff, C. H., Liljestrom, P. & Schlesinger, M. J. (1995). The 6-kilodalton membrane protein of Semliki Forest virus is involved in the budding process. *J Virol* **69**, 469-75.
Lusa, S., Garoff, H. & Liljestrom, P. (1991). Fate of the 6K membrane protein of Semliki Forest virus during virus assembly. *Virology* **185**, 843-6.
Mancini, E. J., Clarke, M., Gowen, B. E., Rutten, T. & Fuller, S. D. (2000). Cryo-electron microscopy reveals the functional organization of an enveloped virus, Semliki Forest virus. *Mol Cell* **5**, 255-66.
Mason, J. T. & O'Leary, T. J. (1991). Effects of formaldehyde fixation on protein secondary structure: a calorimetric and infrared spectroscopic investigation. *J Histochem Cytochem* **39**, 225-9.
Mayne, J. T., Rice, C. M., Strauss, E. G., Hunkapiller, M. W. & Strauss, J. H. (1984). Biochemical studies of the maturation of the small Sindbis virus glycoprotein E3. *Virology* **134**, 338-57.
McInerney, G. M., Smit, J. M., Liljestrom, P. & Wilschut, J. (2004). Semliki Forest virus produced in the absence of the 6K protein has an altered spike structure as revealed by decreased membrane fusion capacity. *Virology* **325**, 200-6.
Melancon, P. & Garoff, H. (1987). Processing of the Semliki Forest virus structural polyprotein: role of the capsid protease. *J Virol* **61**, 1301-9.

Metz, B., Kersten, G. F., Hoogerhout, P., Brugghe, H. F., Timmermans, H. A., de Jong, A., Meiring, H., ten Hove, J., Hennink, W. E., Crommelin, D. J. & Jiskoot, W. (2004). Identification of formaldehyde-induced modifications in proteins: reactions with model peptides. *J Biol Chem* **279**, 6235-43.

Modis, Y., Ogata, S., Clements, D. & Harrison, S. C. (2004). Structure of the dengue virus envelope protein after membrane fusion. *Nature* **427**, 313-9.

Mukhopadhyay, S., Zhang, W., Gabler, S., Chipman, P. R., Strauss, E. G., Strauss, J. H., Baker, T. S., Kuhn, R. J. & Rossmann, M. G. (2006). Mapping the structure and function of the E1 and E2 glycoproteins in alphaviruses. *Structure* **14**, 63-73.

Nyfeler, S., Senn, K. & Kempf, C. (2001). Expression of Semliki Forest virus E1 protein in Escherichia coli. Low pH-induced pore formation. *J Biol Chem* **276**, 15453-7.

Oldstone, M. B., Tishon, A., Dutko, F. J., Kennedy, S. I., Holland, J. J. & Lampert, P. W. (1980). Does the major histocompatibility complex serve as a specific receptor for Semliki Forest virus? *J Virol* **34**, 256-65.

Owen, K. E. & Kuhn, R. J. (1996). Identification of a region in the Sindbis virus nucleocapsid protein that is involved in specificity of RNA encapsidation. *J Virol* **70**, 2757-63.

Paredes, A. M., Ferreira, D., Horton, M., Saad, A., Tsuruta, H., Johnston, R., Klimstra, W., Ryman, K., Hernandez, R., Chiu, W. & Brown, D. T. (2004). Conformational changes in Sindbis virions resulting from exposure to low pH and interactions with cells suggest that cell penetration may occur at the cell surface in the absence of membrane fusion. *Virology* **324**, 373-86.

Paredes, A. M., Heidner, H., Thuman-Commike, P., Prasad, B. V., Johnston, R. E. & Chiu, W. (1998). Structural localization of the E3 glycoprotein in attenuated Sindbis virus mutants. *J Virol* **72**, 1534-41.

Peranen, J. & Kaariainen, L. (1991). Biogenesis of type I cytopathic vacuoles in Semliki Forest virus-infected BHK cells. *J Virol* **65**, 1623-7.

Phalen, T. & Kielian, M. (1991). Cholesterol is required for infection by Semliki Forest virus. *J Cell Biol* **112**, 615-23.

Pletnev, S. V., Zhang, W., Mukhopadhyay, S., Fisher, B. R., Hernandez, R., Brown, D. T., Baker, T. S., Rossmann, M. G. & Kuhn, R. J. (2001). Locations of carbohydrate sites on alphavirus glycoproteins show that E1 forms an icosahedral scaffold. *Cell* **105**, 127-36.

Puchtler, H. & Meloan, S. N. (1985). On the chemistry of formaldehyde fixation and its effects on immunohistochemical reactions. *Histochemistry* **82**, 201-4.

Rey, F. A., Heinz, F. X., Mandl, C., Kunz, C. & Harrison, S. C. (1995). The envelope glycoprotein from tick-borne encephalitis virus at 2 A resolution. *Nature* **375**, 291-8.

Rossmann, M. G. (2000). Fitting atomic models into electron-microscopy maps. *Acta Crystallogr D Biol Crystallogr* **56**, 1341-9.

Roussel, A., Lescar, J., Vaney, M. C., Wengler, G. & Rey, F. A. (2006). Structure and interactions at the viral surface of the envelope protein E1 of semliki forest virus. *Structure* **14**, 75-86.

Salminen, A., Wahlberg, J. M., Lobigs, M., Liljestrom, P. & Garoff, H. (1992). Membrane fusion process of Semliki Forest virus. II: Cleavage-dependent reorganization of the spike protein complex controls virus entry. *J Cell Biol* **116**, 349-57.

Schlesinger, S. & Schlesinger, M. J. (2001). Fields Virology, 4th edn, pp. 895-910. Edited by D. M. Knipe & P. M. Howley: Lippincott Williams & Wilkins.

Schmidt, M. F., Bracha, M. & Schlesinger, M. J. (1979). Evidence for covalent attachment of fatty acids to Sindbis virus glycoproteins. *Proc Natl Acad Sci U S A* **76**, 1687-91.

Shope, R. E. (1980). Medical significance of Togaviruses: An overview of diseases caused by Togaviruses in man and in domestic and wild vertebrate animals. *The Togaviruses: Biology, Structure, Replication*, 47-77.

Simons, K. & Garoff, H. (1980). The budding mechanisms of enveloped animal viruses. *J Gen Virol* **50**, 1-21.

Simons, K., Garoff, H. & Helenius, A. (1982). How an animal virus gets into and out of its host cell. *Sci Am* **246**, 58-66.
Singh, I. & Helenius, A. (1992). Role of ribosomes in Semliki Forest virus nucleocapsid uncoating. *J Virol* **66**, 7049-58.
Skehel, J. J. & Wiley, D. C. (2000). Receptor binding and membrane fusion in virus entry: the influenza hemagglutinin. *Annu Rev Biochem* **69**, 531-69.
Skoging, U. & Liljestrom, P. (1998). Role of the C-terminal tryptophan residue for the structure-function of the alphavirus capsid protein. *J Mol Biol* **279**, 865-72.
Skoging, U., Vihinen, M., Nilsson, L. & Liljestrom, P. (1996). Aromatic interactions define the binding of the alphavirus spike to its nucleocapsid. *Structure* **4**, 519-29.
Skoging-Nyberg, U. & Liljestrom, P. (2000). A conserved leucine in the cytoplasmic domain of the Semliki Forest virus spike protein is important for budding. *Arch Virol* **145**, 1225-30.
Skoging-Nyberg, U. & Liljestrom, P. (2001). M-X-I motif of semliki forest virus capsid protein affects nucleocapsid assembly. *J Virol* **75**, 4625-32.
Smith, A. E. & Helenius, A. (2004). How viruses enter animal cells. *Science* **304**, 237-42.
Smith, T. J., Cheng, R. H., Olson, N. H., Peterson, P., Chase, E., Kuhn, R. J. & Baker, T. S. (1995). Putative receptor binding sites on alphaviruses as visualized by cryoelectron microscopy. *Proc Natl Acad Sci U S A* **92**, 10648-52.
Sofer, G. (2002-2003). Inactivation of viruses. *BioPharm International*.
Strauss, J. H. & Strauss, E. G. (1994). The alphaviruses: gene expression, replication, and evolution. *Microbiol Rev* **58**, 491-562.
Strauss, J. H., Strauss, E. G. & Kuhn, R. J. (1995). Budding of alphaviruses. *Trends Microbiol* **3**, 346-50.
Tubulekas, I. & Liljestrom, P. (1998). Suppressors of cleavage-site mutations in the p62 envelope protein of Semliki Forest virus reveal dynamics in spike structure and function. *J Virol* **72**, 2825-31.
Wahlberg, J. M., Boere, W. A. & Garoff, H. (1989). The heterodimeric association between the membrane proteins of Semliki Forest virus changes its sensitivity to low pH during virus maturation. *J Virol* **63**, 4991-7.
Wahlberg, J. M., Bron, R., Wilschut, J. & Garoff, H. (1992). Membrane fusion of Semliki Forest virus involves homotrimers of the fusion protein. *J Virol* **66**, 7309-18.
Wahlberg, J. M. & Garoff, H. (1992). Membrane fusion process of Semliki Forest virus. I: Low pH-induced rearrangement in spike protein quaternary structure precedes virus penetration into cells. *J Cell Biol* **116**, 339-48.
Wang, K. S., Kuhn, R. J., Strauss, E. G., Ou, S. & Strauss, J. H. (1992). High-affinity laminin receptor is a receptor for Sindbis virus in mammalian cells. *J Virol* **66**, 4992-5001.
Weiss, B., Geigenmuller-Gnirke, U. & Schlesinger, S. (1994). Interactions between Sindbis virus RNAs and a 68 amino acid derivative of the viral capsid protein further defines the capsid binding site. *Nucleic Acids Res* **22**, 780-6.
Weiss, B., Nitschko, H., Ghattas, I., Wright, R. & Schlesinger, S. (1989). Evidence for specificity in the encapsidation of Sindbis virus RNAs. *J Virol* **63**, 5310-8.
Weissenhorn, W., Dessen, A., Calder, L. J., Harrison, S. C., Skehel, J. J. & Wiley, D. C. (1999). Structural basis for membrane fusion by enveloped viruses. *Mol Membr Biol* **16**, 3-9.
Welch, W. J. & Sefton, B. M. (1979). Two small virus-specific polypeptides are produced during infection with Sindbis virus. *J Virol* **29**, 1186-95.
Wengler, G. (1984). Identification of a transfer of viral core protein to cellular ribosomes during the early stages of alphavirus infection. *Virology* **134**, 435-42.
Wengler, G. & Rey, F. A. (1999). The isolation of the ectodomain of the alphavirus E1 protein as a soluble hemagglutinin and its crystallization. *Virology* **257**, 472-82.
White, J. & Helenius, A. (1980a). pH-dependent fusion between the Semliki Forest virus membrane and liposomes. *Proc Natl Acad Sci U S A* **77**, 3273-7.
White, J. & Helenius, A. (1980b). pH-dependent fusion between the Semliki Forest virus membrane and liposomes. *Proc. Natl. Acad. Sci. USA* **77**, 3273-3277.

White, J., Kartenbeck, J. & Helenius, A. (1980). Fusion of Semliki forest virus with the plasma membrane can be induced by low pH. *J Cell Biol* **87**, 264-72.
Wiley, D. C. & Skehel, J. J. (1987). The structure and function of the hemagglutinin membrane glycoprotein of influenza virus. *Annu Rev Biochem* **56**, 365-94.
Wilschut, J., Corver, J., Nieva, J. L., Bron, R., Moesby, L., Reddy, K. C. & Bittman, R. (1995). Fusion of Semliki Forest virus with cholesterol-containing liposomes at low pH: a specific requirement for sphingolipids. *Mol Membr Biol* **12**, 143-9.
Wilson, I. A., Skehel, J. J. & Wiley, D. C. (1981). Structure of the haemagglutinin membrane glycoprotein of influenza virus at 3 A resolution. *Nature* **289**, 366-73.
Zaitseva, E., Mittal, A., Griffin, D. E. & Chernomordik, L. V. (2005). Class II fusion protein of alphaviruses drives membrane fusion through the same pathway as class I proteins. *J Cell Biol* **169**, 167-77.
Zhang, W., Fisher, B. R., Olson, N. H., Strauss, J. H., Kuhn, R. J. & Baker, T. S. (2002a). Aura virus structure suggests that the T=4 organization is a fundamental property of viral structural proteins. *J Virol* **76**, 7239-46.
Zhang, W., Heil, M., Kuhn, R. J. & Baker, T. S. (2005). Heparin binding sites on Ross River virus revealed by electron cryo-microscopy. *Virology* **332**, 511-8.
Zhang, W., Mukhopadhyay, S., Pletnev, S. V., Baker, T. S., Kuhn, R. J. & Rossmann, M. G. (2002b). Placement of the structural proteins in Sindbis virus. *J Virol* **76**, 11645-58.
Zhang, X., Fugere, M., Day, R. & Kielian, M. (2003). Furin processing and proteolytic activation of Semliki Forest virus. *J Virol* **77**, 2981-9.
Zhao, H., Lindqvist, B., Garoff, H., von Bonsdorff, C. H. & Liljestrom, P. (1994). A tyrosine-based motif in the cytoplasmic domain of the alphavirus envelope protein is essential for budding. *Embo J* **13**, 4204-11.
Ziemiecki, A. & Garoff, H. (1978). Subunit composition of the membrane glycoprotein complex of Semliki Forest virus. *J Mol Biol* **122**, 259-69.
Ziemiecki, A., Garoff, H. & Simons, K. (1980). Formation of the Semliki Forest virus membrane glycoprotein complexes in the infected cell. *J Gen Virol* **50**, 111-23.